Study of Low Flow Rate Ladle Bottom Gas Stirring Using Triaxial Vibration Signals

Jaefer Yenus[1]*, Geoffrey Brooks[1], Michelle Dunn[1], Zushu Li[2], Tim Goodwin[3]

[1]Swinburne University of Technology, Hawthorn, VIC 3122, Australia

[2]University of Warwick, Coventry CV4 7AL, UK

[3]Tata Steel, Aldwarke Lane Rotherham S60 1DW, UK

*Corresponding author, Email: jyenus@swin.edu.au , Phone: +61392145473

Abstract

Secondary steelmaking plays a great role in enhancing the quality of the final steel product. The metal quality is a function of metal bath stirring in ladles. The metal bath is often stirred by an inert gas to achieve maximum compositional and thermal uniformity throughout the melt. Ladle operators often observe the top surface phenomena such as level of meniscus disturbance to evaluate the status of stirring. However, this type of monitoring has significant limitations in assessing the process accurately especially at low gas flow rate bubbling. The present study investigates stirring phenomena using ladle wall triaxial vibration at a low flow rate on a steel-made laboratory model and plant scale for the case of vacuum tank degasser. Cold model and plant data were successfully modelled by partial least square regression to predict the amount of stirring. In the cold model, it was found that the combined vibration signal could predict the stirring power and recirculation speed effectively in specific frequency ranges. Plant trials also revealed that there is a high structure in each dataset and in the same frequency ranges at the water model. In the case of industrial data, the degree of linear relationship was strong for data taken from a single heat.

1 Introduction

The steel melt poured to continuous casting operations should maintain a minimum temperature and chemical composition stratification as well as have its impurities absorbed thoroughly to improve the quality of the final product. This is achieved by stirring molten steel by a pressurized argon gas in ladles. Low gas flow rates are intended to rinse the steel and attain thermal and/or chemical homogenization while intense stirring is often practised to facilitate slag-metal reactions.[1-3] Hence, monitoring the status of the stirring is important in attaining the desired quality as well as in optimizing argon gas consumption.

Leaks in the argon supply system, variable back pressure because of variable plug conditions and resistance to flow are some of the difficulties facing ladle operators in precisely evaluating stirring status at low volumetric gas flow rates.[2, 4] Efforts are underway to detect ladle wall vibration due to gas injection to explain the level of agitation inside.[5-16] Mucciardi[17] used an accelerometer to measure ladle vibration due to stirring to correlate the mixing power and vibration signal. He reported that an accelerometer is a viable transducer for controlling the interaction between liquids and gases when direct contact with the liquid phase is not practical. Minion et al. [7] developed vibration signal based monitoring technique for ladle stirring. Kemeny and his co-researchers developed commercial sensors based on ladle vibration to predict the degree of stirring.[8] Vibration based control system (TruStir) developed by Nupro Corporation was implemented in various steel plants such as Hadeed[14] and Dongbu[16]. It was reported that the monitoring system improved steel cleanliness and reduced argon consumption.[14] Others like Burty et al.[9-11],Yuri et al. [12] and Kostetskii et al.[18] have measured vibration, sound and/or ladle eye size both on industrial and laboratory scales to characterize the stirring process. Xu et

al. used a different approach by combining the vibration, bubbling sound and ladle eye size to find the latent variable to predict the stirring power.[4] However, detecting the stirring status at low flow rates as well as the effect of sensor location is not fully understood. The authors of this paper previously studied bottom gas stirring at different flow rate ranges in plastic-walled water model using triaxial vibration. They discovered specific informative frequency ranges that correspond to each flow rate range. They also investigated the effect of accelerometer location on the vessel external wall. They reported that sensor location does not change the amount of the information but does influence the location of the frequency ranges.[5-6] The result was not verified by industrial data or for different ladle capacities and configuration.

This study focuses on investigating the low gas flow rate-stirring phenomenon using triaxial vibration in vacuum tank degasser using laboratory and plant data. In the lab-scale study, a steel-made water model that incorporates ladle supports and tank was used. The study began by selecting the optimum sensor location in the cold model using principal component analysis (PCA) and then applied partial least square regression for a water model and plant data to develop a correlation between the process parameters and a vibration signal.

2 Methodology

2.1 Physical Modelling

The method of study was experimental. It involved vibration measurement from an air stirred water model and an argon stirred industrial ladle. The physical cold model was built from stainless steel and its shape was slightly tapered cylindrical as the industrial ladle. This was aimed at maintaining similar vibration response in both scales. Since plant working conditions related to temperature and visual obscurity of liquid metal and the size of industrial reactors make it difficult for carrying out direct and extensive experimental study, a lab-scale physical cold model has been built to analyze the stirring process. [3, 19] The use of scaled down models is advantageous in studying the process by varying process parameters and is relatively cheap. [20] Physical cold models are based on geometric and dynamic similarities. Geometric similarity refers mainly to the shape of the industrial reactor and its bath height whereas the dynamic similarity is related to the forces acting on laboratory and full scales. However, it is difficult to achieve complete geometric and dynamic similarities in physical models.[20] The shape of the industrial reactor may change with time due to erosion and solidification of metal. To achieve similar ratios of corresponding forces (such as pressure, inertial, gravitational, and viscous) between the model and the full-scale systems, equivalence of the dimensionless numbers(Reynolds and the Froude number) must be maintained.[21] However, for scaled down water models it is impossible to respect both similarities at the same time.[21] Froude number similarity criterion was used in this study because isothermal flow phenomena in gas stirred ladles are dominated by inertial and gravitational/buoyancy forces. Mazumdar and his co-researchers built the relationship between operating gas flow rates in the model and full-scale systems based on these concepts.[3, 22] Irons et al. have also applied similar concepts to derive the dynamic similarities between the plant and laboratory scales.[23] For geometrically and dynamically similar gas stirred systems, volumetric gas flow rates can be correlated by the following relationship. [21, 23]

$$Q_m = \lambda^{2.5} Q_f \quad (1)$$

Where f and m represent full and laboratory model scales respectively. A scale factor (λ) of 0.1 was used in order to have Froude dominated turbulent flow in the model (i.e. similar to gas stirred ladles). Water and oil (ρ=850 kg /m^3) were used to simulate molten steel and slag respectively. The selection of water is due to its kinematic similarity with molten steel at working

temperature, easy availability and being widely used in cold model steelmaking studies. [20] However, the physical and dynamic property of slag is highly variable and is difficult to mimic it with a single material. Though oil does not perfectly simulate slag, its floatability on water, availability, and being widely used by other steelmaking researchers, make it an optimal choice for this study. [5-6, 9-10, 22, 24-26] While oil and water are not ideal liquids to mimic iron and slag, they provide a reasonable basis by which to model the behavior of an industrial system for collecting data in various experimental conditions.

2.2 Analysis Technique

The main analysis methods used in this study were linear PCA and PLS. PCA a multivariate statistical technique that is simple, non-parametric method of mining relevant information from large data sets. PLS is a multivariate statistical technique used to find the correlation between input and output matrices by projecting the predicted variables and the observable variables to a new space. The choice of PLS was due to its ability to handle extraneous, collinear and missing data. Another essential characteristic of PLS is its accuracy improves with more observations. The selection PCA based on its reliability and ability to detect the structure in a large dataset. Hence, highly structured data means the N-dimensional data can be projected to a single viewpoint that is most informative. Both PLS and PCA are simple and convenient for online monitoring. These techniques also have good success stories in industrial multivariate monitoring.[27-32] Both techniques have been widely used in understanding the behaviour of an industrial process by extracting the significant hidden features in the process data.[33] However, these techniques have limited capability in revealing nonlinear characteristics in the dataset.

Principal component analysis (PCA) is a statistical procedure that was developed by Pearson in 1901.[34] It delivers a roadmap for how to reduce a complex set of data to a lower dimension to disclose the hidden and simplified structure that often underlies it. Mathematically if '$\boldsymbol{X}$' is the original dataset matrix and '$\boldsymbol{Y}$' is the new transformed matrix of the original dataset, then the goal of PCA is to find orthonormal matrix $\boldsymbol{G}$ in Equation 2.

$$\boldsymbol{Y} = \boldsymbol{PX} \qquad 2$$

The rows of $\boldsymbol{P}$ are the principal components of $\boldsymbol{X}$.[32] If $\boldsymbol{Y}$ has k variables with n observations, for mean-centered and scaled data $\boldsymbol{X}$, the first principal component $PC1$ is a linear combination of $\boldsymbol{Y}$ and the loading vector of $\boldsymbol{Y}$, w_1 ($\boldsymbol{PC1} = \boldsymbol{Yw_1}$). $PC1$ has the greatest variance with a precondition of $|\boldsymbol{w1}| = 1$. $PC2$, second principal component, is computed in similar manner as PC1 and has the next maximum variance that fulfils $|\boldsymbol{w2}| = 1$. The loading vectors $\boldsymbol{w_i}$ are the eigenvectors of the covariance matrix of, $((n-1)^{-1}Y^TY)$. [27] Principal components are uncorrelated to each other and are sorted such that the k^{th} PC has bigger value than the next. It is a reliable, simple and nonparametric method of extracting important information from a large dataset. It has simple mathematical operations, which make it convenient for online analysis. The basic concept of PCA is shown schematically in Figure 1.[27] Assume that there are five variables in a process. During a time period, the variables x_1, x_3 and x_4 exhibit the same

pattern for a certain disturbance. This shows these variables are correlated with each other for this time interval. Variables x_2 and x_5 exhibit a similar pattern but different to the first. x_2 and x_5 are correlated with each other but not correlated to x_1, x_3 and x_4. The first PC is a weighted average of x_1, x_3 and x_4, while the second component is a weighted average of x_2 and x_5. Detail description of this technique can be found in the literature.[27, 32, 35-37] In this investigation, three variables make the state matrix, $\boldsymbol{Y}$ which is the input for PCA. In this study acceleration are measured in the x, y and z directions. The goal was to linearly combine and suppress them to one or two latent variables that can describe most of the stirring process variation. The latent variables were then used to identify the most informative frequency ranges.

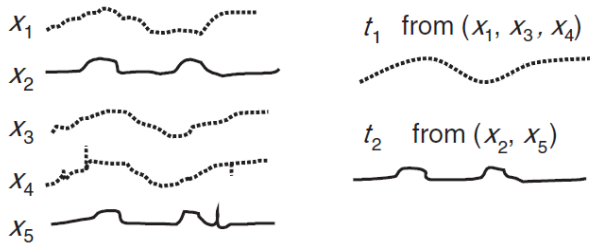

Figure 1 A simplified representation of PCA [27]

The limitation with PCA is that it only deals with a single data matrix (i.e. input or output) at a time. To consider input and output datasets simultaneously for discovering the relationship, PLS is a key tool. PLS model deals with the variation in input as well as output space simultaneously. [27, 30] It is essentially useful when a set of dependent variables are required to be predicted from a significant number of independent variables known as predictors. [38] This multivariate statistical technique has the ability to handle data that are noisy, collinear or data with incomplete variables in both dependent and independent sets. Another outstanding characteristic of PLS is that the accuracy of its model parameters can be enhanced by increasing the number of relevant observations and variables. These all make it an ideal choice to handle industrial data. PLS decomposes normalized and column centred matrices $\boldsymbol{X}$ $(\boldsymbol{nxk})$ and $\boldsymbol{Y}$ $(\boldsymbol{nxm})$ into scores and loading matrices shown in Equations 3 and 4. [39]

$$X = TP' + E \tag{3}$$

$$Y = UQ' + F \tag{4}$$

where $T(nxA)$ and $U(nxA)$ are the latent variable scores and $P(kxA)$ and $Q(mxA)$ are loading matrices. E and F are residual matrices. A simplified clarification of PLS is given by Figure 2. There are five input variables X_1, X_2, X_3, X_4 and X_5 and one output variable y_1. If the change in X_2 and X_5 also affects the product quality y_1 at same time period, the variation in y_1 is probably related to variation in X_2 and X_5. In this scenario, the first latent variable t_1 is a weighted average of X_2 and X_5 whose circumstances best describes y_1.[27] Detail description of PLS can be found in the literature.[27, 30-31, 38]

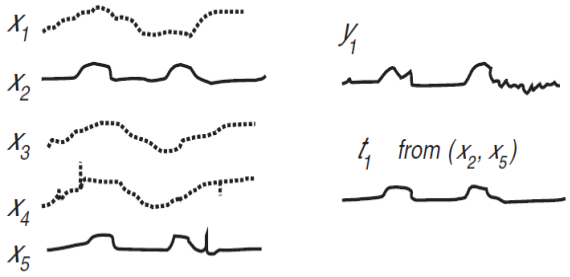

Figure 2 Schematic representation of PLS[27]

In this study, the input variables ($\boldsymbol{X}$) are flow rate, water height, and oil depth while the output variables ($\boldsymbol{Y}$) are the vibration signals along the three axes. PLS was applied for the selected highly structured frequency ranges. The overall analysis strategy is shown in Figure 3. Figure 3 shows the input matrix for PCA is the vibration (x, y and z). In similar manner, Figure 3 shows the input/predictor matrix and output/response matrix for PLS analysis. The input matrix consists volumetric gas flow rate,Q, the bottom layer depth (H) and top layer thickness (h) where as the output matrix contain the vibration in three axes.

As the plant data are noisy, the frequency ranges where the power of the signal is concentrated were analyzed using the Short Time Fast Fourier Transform (STFT). The short time Fourier Transform is a Fourier-related transform that can convert non-stationary one-dimensional time signal to the two-dimensional frequency-time domain. Mathematically it is defined by Equation 5.[40]

$$TF(t,f) = \left|\int_{-\infty}^{+\infty} y(\tau)h(\tau - t)e^{-i2\pi f\tau}d\tau\right| \quad (5)$$

where $h(t)$ is a short-time analysis window centred at $t = 0$. Furthermore, to capture essential patterns and improve the signal to noise ratio without greatly destroying the signal, the plant data were smoothed using Savitzky-Golay filter (S-G filter). S-G filter is the most widely used filter for smoothing data.[41] It smooths data using a local least squares (LS) polynomial approximation. [42] It acts on a vector of input samples $x(k)$ to give a smoothed vector of $Y(k)$. This filter is defined by Equation 6.[43]

$$\mathrm{Y_j} = \sum_{\mathrm{i}=-\frac{\mathrm{m}-1}{2}}^{\mathrm{i}=\frac{\mathrm{m}-1}{2}} \mathrm{C_i}\,\mathrm{Y_{j+i}} \quad , \quad \frac{\mathrm{m}+1}{2} \leq \mathrm{n} - \frac{\mathrm{m}-1}{2} \quad (6)$$

where n is sample size of the data (X_i, Y_i) and $j = 1, \ldots, n$. m is the number of convolution coefficients ,C_i. In this analysis, the S-G filter in Matlab (Mathworks) is utilized. The window width over which to do the polynomial fit, and the order of the polynomial are chosen in a way that gives the best fit and better correlation between latent variable and process parameters.

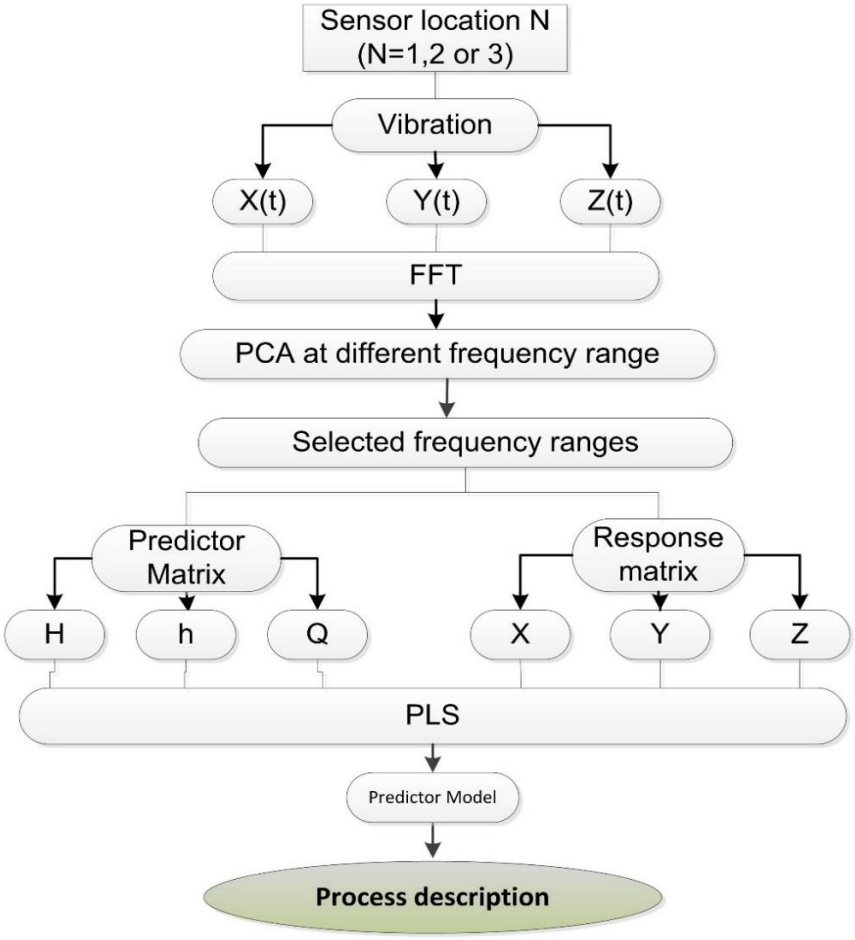

185

186 Figure 3 Overall analysis scheme

2.3 Experiment

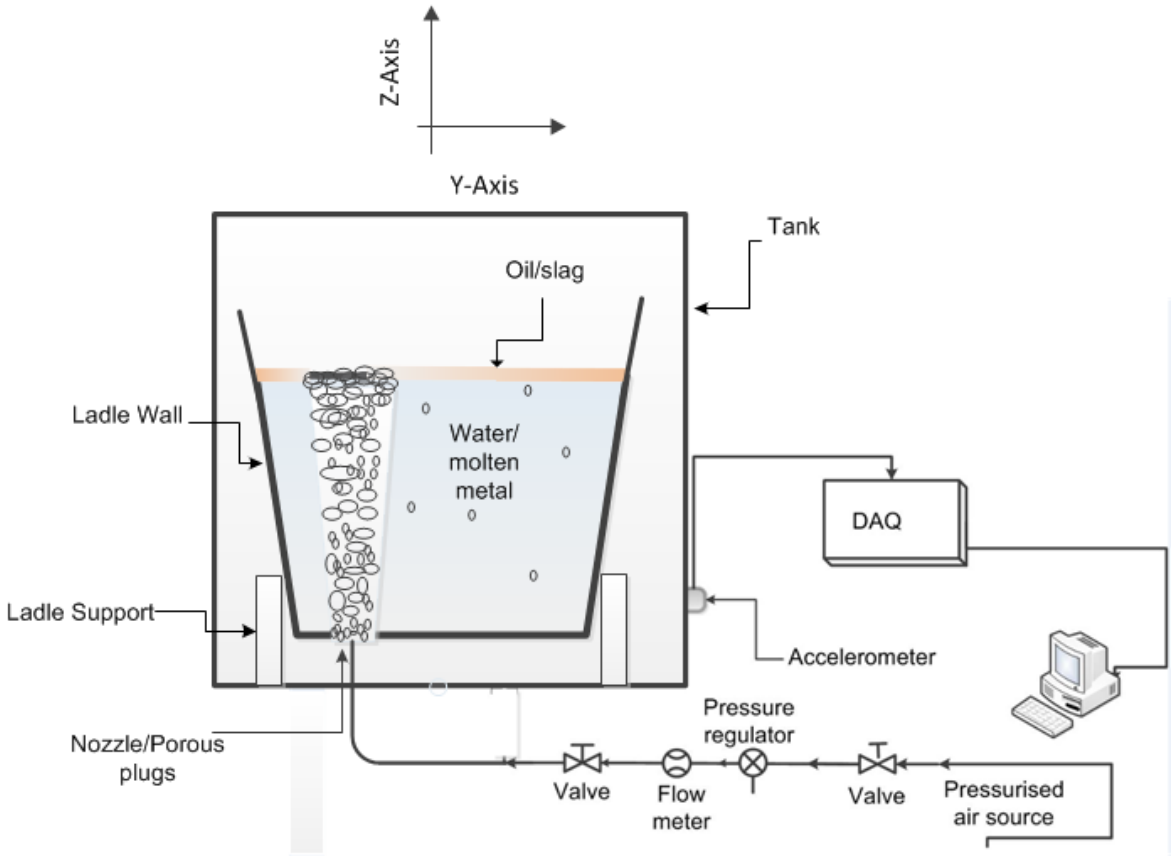

Figure 4 Overall laboratory experimental setup

In the lab-scale study, vibration measurements were carried out on a physical cold model of a 160-tonne capacity industrial ladle shown in Figure 4.The compressed air flow rate was controlled using standard rotameters (±3 and ±5 % full-scale errors). The air pressure was made to be at a fixed value by a pressure regulator at 0.20 Mpa. A stud mounted triaxial accelerometer (95 mv/g sensitivity and ±50 g measurement range) was used for simultaneous multi-axis (x, y, and z) vessel wall vibration measurement. Analog vibration data coming from the accelerometer was digitized using a 4-channel C series dynamic signal acquisition module (NI 9234) before it was exported to a computer. National Instrument SignalExpresss 2013 software was used to acquire, generate and save signals. The vessel frame was tightly fixed to the concrete floor to make background noise negligible. A sample time of 6 seconds was taken throughout the experiment because it had been observed that reducing the sample time to 6 seconds resulted in no reduction of the quality of the data.[5-6] The sampling frequency of the accelerometer was taken to be 1828Hz to avoid any aliasing. The sensor locations considered in this study are the ladle wall, the ladle support, and the tank external wall. Data were gathered from each location at a time using identical experimental conditions.

In the plant, the study was carried out on a Vacuum Tank Degasser (VTD) operated by Tata Steel that is used to homogenize the liquid steel bath temperature and composition and to reduce the concentrations of dissolved gasses in the liquid steel. The basic configuration and shape of the VTD look like the sketch in Figure 4. The gas was injected through two sidewall porous plugs at the bottom of a 160-tonne ladle. The accelerometer was placed on the external

wall of the tank and same DAQ instruments were used to acquire data. Vibration measured from six heats were studied individually and in combination. One heat is defined as one ladle operation. During plant vibration measurement, the amount of metal and slag, plug life, plug position, barrel life and slag line life were different in the considered heats. The barrel and slagline are distinct parts of the ladle lining. The slagline is a slightly thicker lined part of the lining around the height of the steelmaking slag. This wears more rapidly than the rest of the ladle lining lower down, which is known as the barrel. The number of lives of each is simply the number of heats which have been in contact with the ladle slagline and barrel since they were installed. It is common to see a barrel life in excess of the slagline life, as the slagline can be replaced independently of the barrel. Ladle of barrel life number 16 to 21 and slagline number 1 to 4 were used during the data collection. The steel weight generally varied from 130 to 150 tonnes while the slag weight was between 1.8 and 3.6 tonnes. Some heats were carried out with new porous plugs and others with old plugs that served two to four heats. Background noise was also measured in different circumstances when the vacuum degasser was not running. The main purpose is to analyze the noise signal separately in order to understand how it affects the main signal's strength.

During water model experiment, the flow rate was taken in the range of 0.67×10^{-6} to 3.33×10^{-5} m^3/s, bottom layer/water depth was varied from 0.24 to 0.3 m and top layer/oil thickness was varied from 0.005 to 0.02 m.

3 Results and Discussion

3.1 Cold model study results

3.1.1 Accelerometer optimum location

The accelerometer was mounted at three different positions on the steel cold model of the vacuum tank degasser. These locations are on the vessel external wall, on the support and on the tank external wall. Figure 5 shows these locations on the physical cold model. Vibration data were collected for single and double layer bubbling at various volumetric airflow rates at each accelerometer location. The datasets from each location were analysed in the time domain and in the frequency domain. To choose optimum sensor location, PCA analysis was carried out in the frequency domain to compare the underlying relationship among the three candidates. The underlying relationship is explained by the data structure.

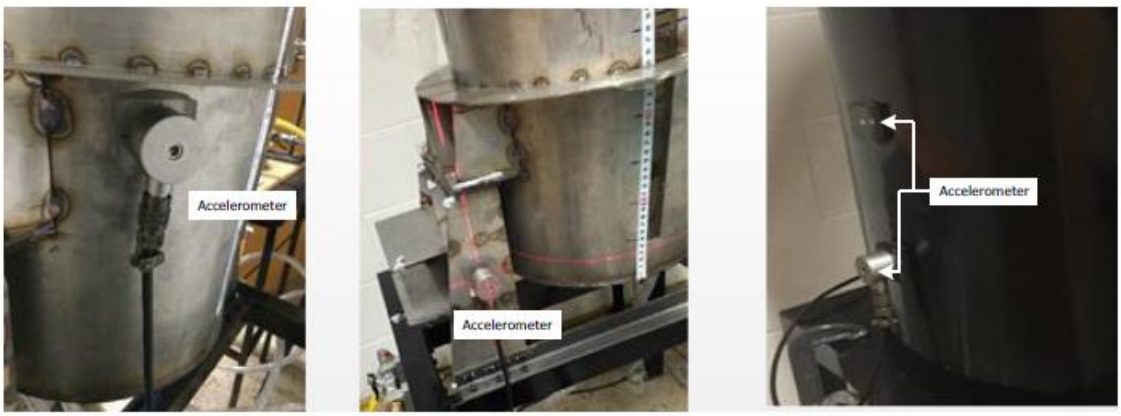

Figure 5 Sensor candidate locations in the laboratory scale

Figure 6 shows the temporal variation of vibration amplitude for the three axes at each location. The result shows that the average vibration along the three axes is not equal when similar axes are compared.

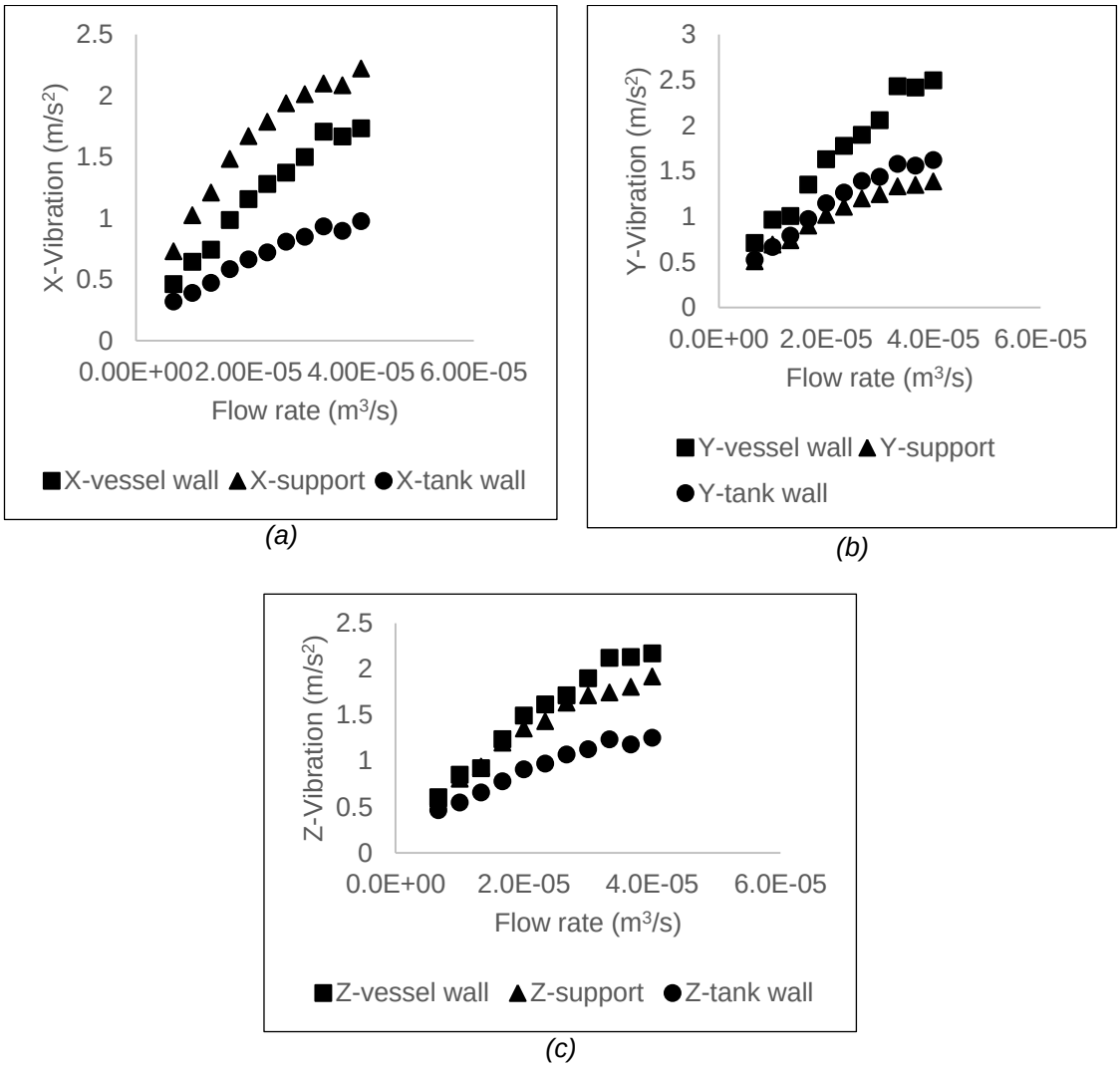

Figure 6 Vibration amplitude versus flow rate in each location for fixed water height and oil depth a) X-axis b) Y-axis c) Z-axis

Furthermore, PCA analysis shows the structures of the data are similar in the three locations. This is shown in Table 1.In Table 1, PC1 values are above 98 % which means PC1 can explain 98 % of the stirring process variation. Only a very small part of this variation is explained by PC2 (=0.5 %). The sum of PC1 and PC2 picks almost all of the information regarding the stirring. Hence, the sensor can be mounted on wall, support or tank as the structure is high in the three positions. This implies that the amount of information of the stirring process of the cold model does not depend on the sensor locations considered in this study. This result is useful in the industry in many ways. It simplifies the difficulty of locating the sensor caused by temperature and accessibility and safety issues. In in the lab-scale and plant scales studies, the accelerometer was mounted on the tank external wall near the support because of easy accessibility and tank surface temperature.

3.1.2 Vibration Analysis in the Selected Location

Vibration data measured while varying the water height, oil depth, and flow rate, was analyzed using principal component analysis (PCA) and partial least square (PLS). To unveil the structure in the data, PCA was used for the whole frequency range. The structure explains how much variation is explained by the first principal component, which is a linear combination of the signals in the three axes. The whole frequency range was subdivided into small frequency ranges and analyzed using PCA to find the frequency range where the structure and the correlation are strong. The analysis result reveals that the data are highly structured in certain frequency ranges. Highly structured data means the data can be projected to a single viewpoint that is most informative. This viewpoint is related to the first principal component. In other words, the first principal component can explain the majority of the variation in the vibration data. As a result, the original three-dimensional (x, y and z) data can be reduced to a single dimension (PC1).To choose one or two frequency ranges, the degree of the linear correlation coefficient (R^2) between different parameters (stirring power (ε), vibration (*V*), bath recirculation speed (U) and flow rate (Q)) and latent variable (PC1) was computed. Table 2 shows the frequency range of their respective values of principal components and R2.

The frequency range 80 to 90 Hz can explain the majority of the variation in the stirring process and the first latent variable computed by combining the vibration signals can linearly predict the stirring power and bath recirculation speed better than the other frequency ranges. Hence, instead of using the whole frequency range, the small frequency range can be used to monitor the stirring process in these flow rates.

With the aim to develop predictive models for stirring status, using vibration signals, the data were analysed within the full and the selected frequency ranges using partial least squares. In Equation 4, $\boldsymbol{X}$ is the predictor, $\boldsymbol{B}$ is regression coefficient and $\boldsymbol{Y_{res}}$ is the residual data.

$$\mathbf{Y} = \mathbf{BX} + \boldsymbol{Y_{res}} \quad (4)$$

Partial least square predicted variable, $\boldsymbol{Y}$, has a strong linear correlation between stirring indicators (stirring power and bath recirculation speed).

Figure 7 shows that the prediction capability of 80-90 Hz frequency range is high. This strengthens the idea that taking the small frequency range can be advantageous and brings no substantial deviation. The stirring power and bath recirculation speed increase linearly with vibration. Figure 7 shows that the slope of the line representing the relationship between vibration and stirring power is higher than that of the bath recirculation speed. This may mean that the rate of linear increase of recirculation with vibration is smaller than the stirring power. Since the recirculation speed better explains the mixing status [7], this relationship may be more descriptive of the actual stirring. In a similar manner, the relationship between flow rate and predicted vibration shown in Figure 8 shows that at fixed bottom layer height, the flow rate can be estimated if the top layer thickness is known. H and h refer to the water height and oil thickness respectively.

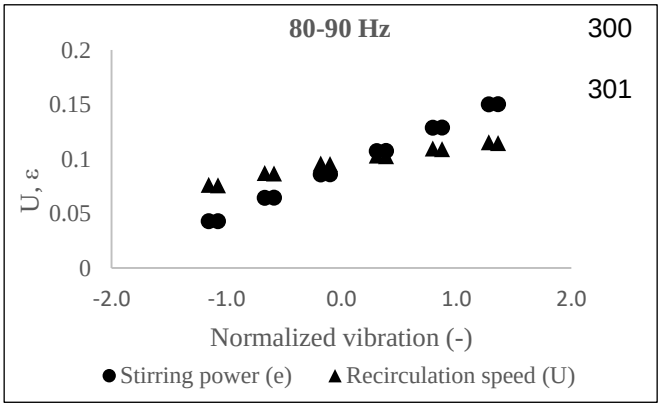

Figure 7 Comparison between stirring power and recirculation speed

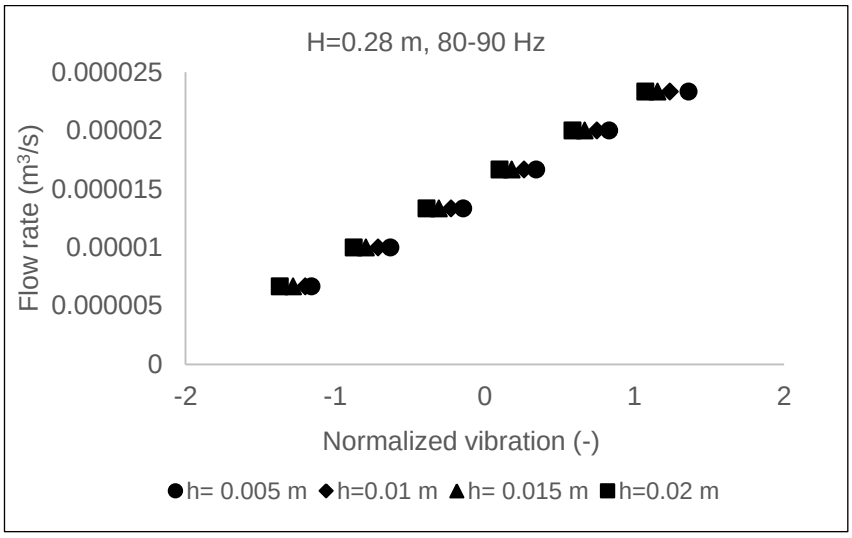

Figure 8 Relationship between flow rate and predicted vibration

3.1.3 Plant Trials

Plant data were collected from a 160-tonne vacuum tank degasser at a Tata Steel plant. The ladle has two porous plugs through which pressurized argon gas was injected. Tank wall vibration at various volumetric gas flow rates was recorded using a triaxial accelerometer mounted on the external tank wall near to supports. Vibration data that correspond to an actual pressure of less than 10 mbar was considered in this investigation. The weight of the molten steel and slag was assumed constant throughout each ladle operation. In addition, vibration from external sources was measured separately in order to know their magnitude and frequency location.

To capture essential patterns and improve the signal to noise ratio without greatly destroying the signal, the plant data were smoothed using the Savitzky-Golay filter (S-G filter).[42] To identify the frequency content of the vibration coming from other sources, Short-Time Fourier Transform (STFT) was applied on data that were measured in the absence of ladle bubbling. This unveils that the power of the noise signal was concentrated on the frequency ranges of between 0 to 50 Hz, 220 to 250 Hz, 500 to 550 Hz and 700 to 800 Hz considering each vibration axis. Consequently, to minimize the effect of this noise signal in the analysis, the data within these frequency ranges have been ignored. Then a similar analysis procedure to the cold model study was followed i.e. PCA was used to uncover the structure and PLS were used to discover the relationship between vibration and stirring status.

Principal component analysis of the vibration data within each heat show that the plant data are highly structured in specific frequency ranges. Table 3 shows the values of the first and second principal components for four heats. Similar results were obtained in the other four heats. These principal components are a combination of the vibration signal in x, y and z-axes.

The data within the frequency ranges in Table 3 were further analyzed by partial least squares to uncover any linear relationship between input variables and the latent variable that is a combination of the three-axis vibration signal. The only input parameter that is assumed to vary throughout the process is the flow rate and hence the variation is mostly related to this parameter. This is demonstrated in Figure 9a which show a strong correlation between the input and output PLS latent variable. Figure 9b shows the linear relationship between predicted vibrations and volumetric flow rate. The frequency range that consistently gives this result is 60 to 70 Hz.

The same procedure was followed to analyze the other heats independently. The result found was similar with slight variation in the degree of correlation. Figure 10 shows the degree of correlation between latent variables of the input and that of the output. The linear relationship is strong. After analyzing each heat individually, the next step was to analyse the combined data to unveil both structure and the relationship. The flow rates were taken from each heat and put in an increasing order. The respective vibration data were then used to construct a state matrix for PCA analysis. The analyses reveal that there is a strong structure in the data in specific frequency ranges.

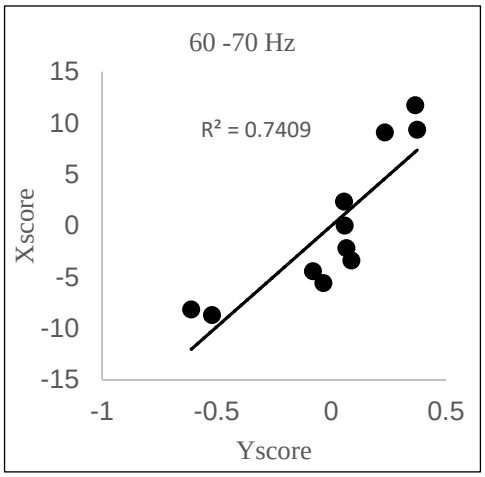

(a)

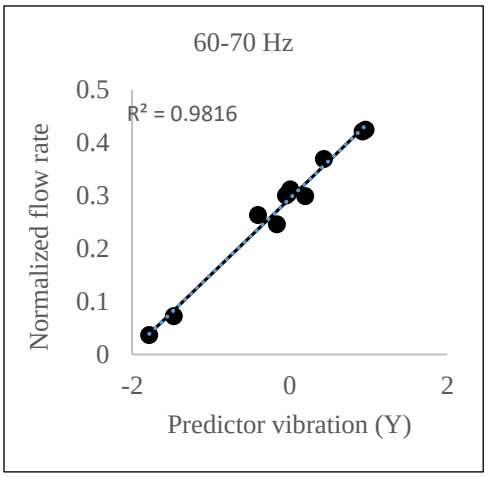

(b)

Figure 9 Relationship between a) input and output latent variables b) flow rate and predicted vibration

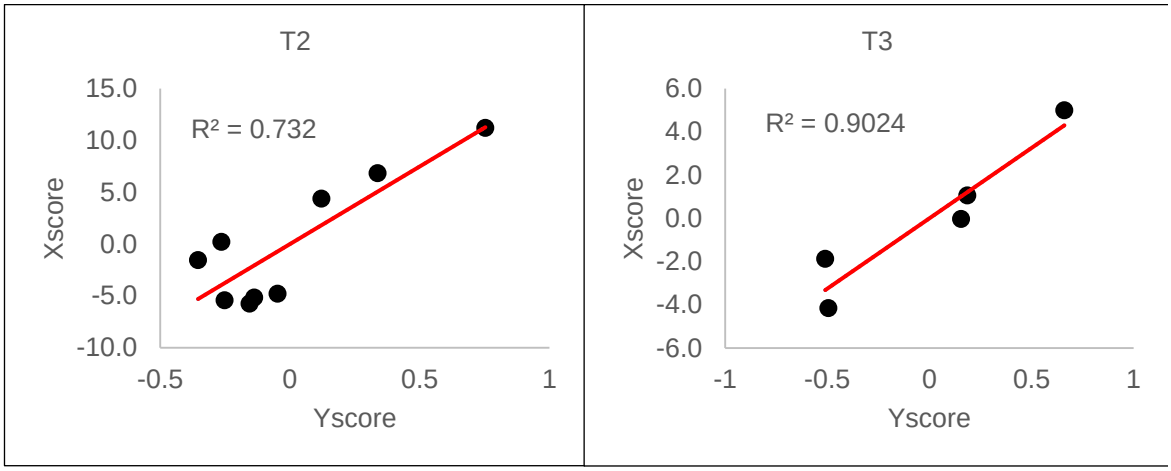

a) b)

Figure 10 Relationship between input and output latent variables in a) T2 and b) T3 heats

To examine the linear relationship between process parameters and vibration signal, the data within these frequency ranges were investigated using partial least square. In Figure 11, the data were taken from six heats. Figure 11 shows that there is no correlation between vibration signal and the flow rate. This disparity could be due to a couple of reasons. Firstly, the underlying relationship could be nonlinear. Secondly, the data come from heats that have different process parameter values such as plug position, plug life, steel weight, slag weight, plug life, and barrel life that can contribute to data scattering due to the size of the data. The steel weight roughly varied from 130 to 150 tonnes while the slag weight was between 1.8 and 3.6 tonnes. In addition, some heats were carried out with new porous plugs and others with old plugs that served from two to four heats. The location of these plugs was also different among the six heats. Hence, the relationship could be improved by carrying out a separate and sufficient plant measurements for each parameter and analyzing the combined data by both linear and nonlinear data analysis techniques. This helps in identifying the effect of each parameters on stirring.

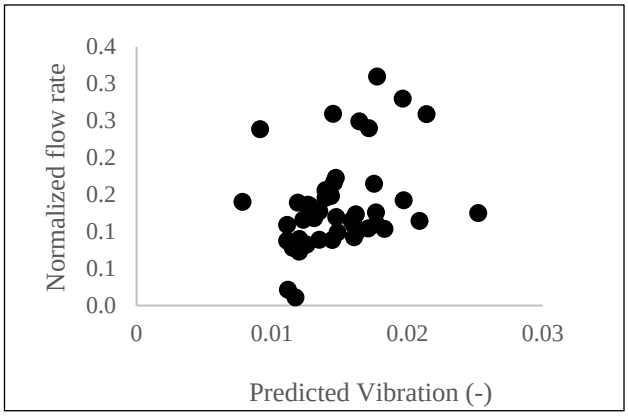

Figure 11 Relationship between flow rate and latent variable

Furthermore, data taken from the six heats were grouped based on similar plug position; steel weight, plug life and slag weight similarities and investigated separately. No sound correlation

was found in each dataset. The other parameters may be still varying and contributing to the scattering of the plant data. The discrepancy may be alleviated by incorporating more plant data and range analysis techniques to determine the underlying relationship and the degree of influence of each parameter.

3.1.4 Comparison of plant and cold-model results

When the results from both data groups are examined, there are similarities and differences. In both cases, the structure is strong and the frequency ranges where this structure resides are the same. These frequency ranges include 60 to 70, 70 to 80, 80 to 90 and 90 to 100 Hz. Table 3 shows the values of the first principal component in cold model and plant data. There is a good agreement between cold model and plant studies concerning the data structure.

The degree of correlation between the latent variables and process parameters in the plant data analysis was comparable to that of the cold model, only for a single heat data in the frequency ranges of 60 to 70 Hz. The plant data in the other frequency ranges show a poor linear relationship. The strong structure identified in the data, however, suggests that further study is needed to discover the underlying relationship.

The water model study indicated that the structure and degree of linear correlation are affected by the variation in the top layer. In the plant scale study, there are additional parameters that are varying from one heat to another. Though the data structure is high, a linear relationship was not found for combined heats.

4 Conclusions

Both cold model and plant scale studies showed that vibration data at low bubbling rates are highly structured when investigated using linear principal component analysis. The three vibration signals in x, y, and z were able to be linearly compressed to a single latent variable. This latent variable explains above 90% of the variation in the vibration data. The frequency ranges where these information lies were in the range of 60 to 70, 70 to 80, 80 to 90 and 90 to 100 Hz. These frequency ranges were consistent in the plant and in water model studies.

The data within these informative frequencies were analyzed by partial least squares to assess the linear relationship between latent variables and process parameters such as flow rate, bottom and top layer depths. The cold model data gave strong linear correlation whereas the investigated plant data show poor linear relationship for most of the cases. Plant data taken from each heat show a comparable degree of linear relationship as the cold model data in the frequency range of 60 to 70 Hz.

Furthermore, the investigation on the optimum sensor location unveils that the amount of information harnessed from the three sensor locations considered in the cold model study is not significantly different. This was an important finding for industrial application. It simplifies the difficulty caused by accessibility, temperature and safety issues. The accelerometer can be mounted on the ladle wall, ladle support or tank without reduction of the amount of information. However, the informative frequency range may shift their location.

To conclude, the cold model data are highly structured and there is a strong linear relationship between vibration and flow rate when the bath level is constant. In addition, the data structure and linear relationships are not affected by accelerometer location. The data are highly structured in the plant as well but variability in plant operations means a separate measurement

of other parameters may be required before the vibration signal can be used as a reliable measurement of stirring.

Acknowledgment

The authors are grateful to Tata Steel for funding this project and people at the industry site for their support during plant measurements.

NOMENCLATURE

H	Water height (meter)
h	Oil depth (meter)
ε	Rate of energy dissipation (watt/t)
$\bar{U}$	Bath recirculation speed (meter/second)
T	Temperature in kelvin
Q	Volumetric gas flow rate (Nm^3/min) Gas flow rate
M	Bath weight (tonne)
P_0	Pressure above the steel bath (bar)
R	Vessel radius (meter)

Reference

1. Ahindra Ghosh: *Secondary steelmaking: principles and applications*. CRC Press, 1st ed.,USA, 2000,pp14-19.
2. Satyendra, "Argon Rinsing of Steels" (2014), http://ispatguru.com/argon-rinsing-of-steels/ Accessed May 2016.
3. Dipak Mazumdar and Roderick IL Guthrie, *ISIJ international ,*1995, vol. 35, pp. 1-1.
4. Xiaodong Xu, Geoffrey A Brooks and William Yang, Metall. Trans. B,2010, vol. 41, pp. 1025-32.
5. Jaefer Yenus, Geoffrey Brooks and Michelle Dunn, Metall. Trans. B, 2016, vol. 47, pp. 2681-89.
6. J Yenus, G Brooks and M Dunn, *APCChE 2015-CHEMECA 2015*, 2015, Australia, pp 2665-76.
7. RL Minion, CF Leckie, KJ Legeard and BD Richardson, *Iron & steelmaker* 1998, vol. 25, pp. 25-31.
8. Francis L Kemeny, David I Walker and Jeremy AT Jones, Google Patents: 2001, pp 1-11.
9. M Burty, C Pussé, DY Sheng, C DANNERT, H KOCHNER, LF SANCHO, J DIAZ, P VALENTIN, C BRUCH and A ARTEAGA, *EUR* 2007, pp. 1-139.
10. M Burty, C Pussé, C Bertoletti, P Wetta and E Cariola, *Revue de Métallurgie* 2006, vol. 103, pp. 493-99.
11. M. Burty, C. Pusse, P. Wetta, F. Sulin, C. Bertoletti, Y. Borneque, D. Pernet and E. Carioli, Google Patents: 2011, pp 1-8.
12. Kostetsky Yuriy, Kukuy David, Kvasov Iluya, Khodyachikh Vadim, Degtyarenko Ilya and Omelchenko Andrey, *METAL 2007: 16 th International Metallurgical and Materials Conference*, 2007, pp 1-7.

13. Frank L Kemeny, DI Walker and J Jones, *58 th Electric Furnace Conference and 17 th Process Technology Conference*, 2000, pp 723-33.
14. N. Behera , A. Wohaishi, R. Subramanian, N. Tewari and R. Bommaraju, *AISTech Conference 2014*, USA, 2014, pp 1423–32.
15. Mika Pylvänäinen, Ville-Valtteri Visuri, Toni Liedes, Jouni Laurila, Konsta Karioja, Sanna Pikkupeura, Seppo Ollila, Timo Fabritius and SSAB Europe Oy, pp.1-9.
16. D. R. Min, C. H. Jung, K. Y. Kim and F. L. Kemeny , AIST 2013, USA, pp. 2075-2081.
17. Frank Mucciardi, *Canadian Metallurgical Quarterly* 1987, vol. 26, pp. 351-57.
18. Yu Kostetskii, I. Kvasov, I. Degtyarenko and D. Kukui, *Russian Metallurgy (Metally)* 2009, vol. 2009, pp. 595-97.
19. D. Guo and G. A. Irons, *Metall. Trans. B,* 2000, vol. 31, pp. 1447-55.
20. Dipak Mazumdar, Modelleing of Steelmaking Process, 1st ed.,CRC Press, USA, 2009, pp 7-15.
21. D. Mazumdar and J. W. Evans, *ISIJ International,* 2004, vol. 44, pp. 447-61.
22. D Mazumdar, HB Kim and RIL Guthrie, *Ironmaking & steelmaking,* 2000, vol. 27, pp. 302-09.
23. K. Krishnapisharody and G. A. Irons, *Metall. Trans. B* 2013, vol. 44, pp. 1486-98.
24. Kimitoshi Yonezawa and Klaus Schwerdtfeger, *ISIJ international,* 2004, vol. 44, pp. 217-19.
25. Krishnakumar Krishnapisharody and GordonA Irons, *Metall. Trans., B* 2006, vol. 37, pp. 763-72.
26. B. X. Xu, Analysis of Bubble Flow in Metallurgical Operations Using Multivariate Statstical techniques, Australia, 2010, p 247.
27. Theodora Kourti, *International Journal of Adaptive Control and Signal Processing,* 2005, vol. 19, pp. 213-46.
28. Theodora Kourti, Jennifer Lee and John F. Macgregor, *Computers & Chemical Engineering,* 1996, vol. 20, pp. S745-S50.
29. J. F. MacGregor and T. Kourti, *Control Engineering Practice,* 1995, vol. 3, pp. 403-14.
30. Svante Wold, Michael Sjöström and Lennart Eriksson, *Chemometrics and Intelligent Laboratory Systems,* 2001, vol. 58, pp. 109-30.
31. Sijmen de Jong, *Chemometrics and Intelligent Laboratory Systems,* 1993, vol. 18, pp. 251-63.
32. Jonathon Shlens, *arXiv preprint arXiv:1404.1100,* 2014, pp.1-13.
33. F. Jia, E. B. Martin and A. J. Morris, *Computers & Chemical Engineering,* 1998, vol. 22, pp. S851-S54.
34. Xueqiang Liu, Xiaoguang Chen, Wenfu Wu and Yaqiu Zhang, *Food control,* 2006, vol. 17, pp. 894-99.
35. Ian Jolliffe, *Encyclopedia of Statistics in Behavioral Science*, John Wiley & Sons, Ltd: 2005.
36. Uwe Kruger and Lei Xie, *Statistical Monitoring of Complex Multivariate Processes: With Applications in Industrial Process Control*,1st ed., John Wiley & Sons, UK, 2012, pp.355-374.
37. Hervé Abdi and Lynne J Williams, *Wiley Interdisciplinary Reviews,:Computational Statistics,* 2010, vol. 2, pp. 433-59.
38. Hervé Abdi, *Encyclopedia for research methods for the social sciences,* 2003, pp. 792-95.
39. Zhiqiang Ge, Chunjie Yang and Zhihuan Song, *Chemical Engineering Science,* 2009, vol. 64, pp. 2245-55.
40. Qingbo He, Jun Wang, Fei Hu and Fanrang Kong, *Journal of Sound and Vibration* 2013, vol. 332, pp. 5635-49.
41. Manfred UA Bromba and Horst Ziegler, *Analytical Chemistry,*1981, vol. 53, pp. 1583-86.

42. S. R. Krishnan and C. S. Seelamantula, *IEEE Transactions on Signal Processing,* 2013, vol. 61, pp. 380-91.
43. Kai Wang, Zhiguo Liu, Gang Liu, Longtao Yi, Kui Yang, Shiqi Peng and Man Chen, *Shock and Vibration,* 2015, pp233-278.

List of Figures

List of Tables

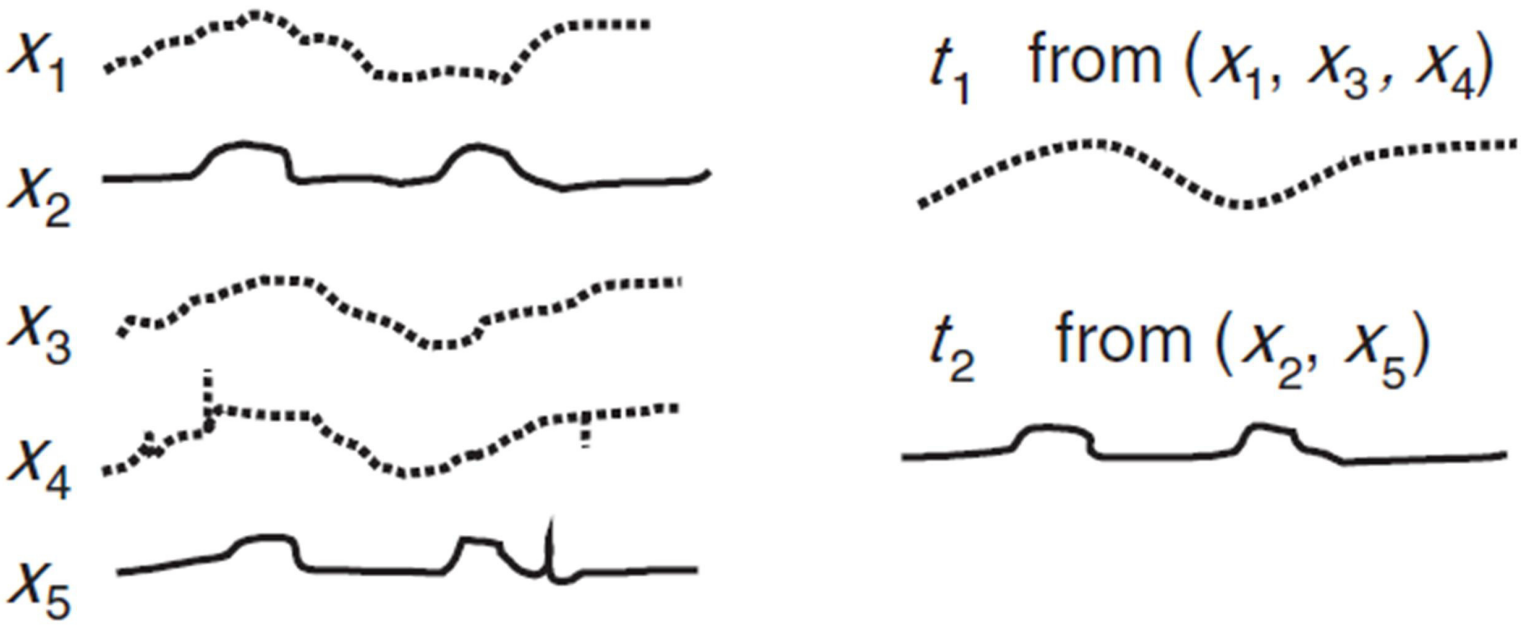

PRINCIPAL COMPONENTS (PCA)

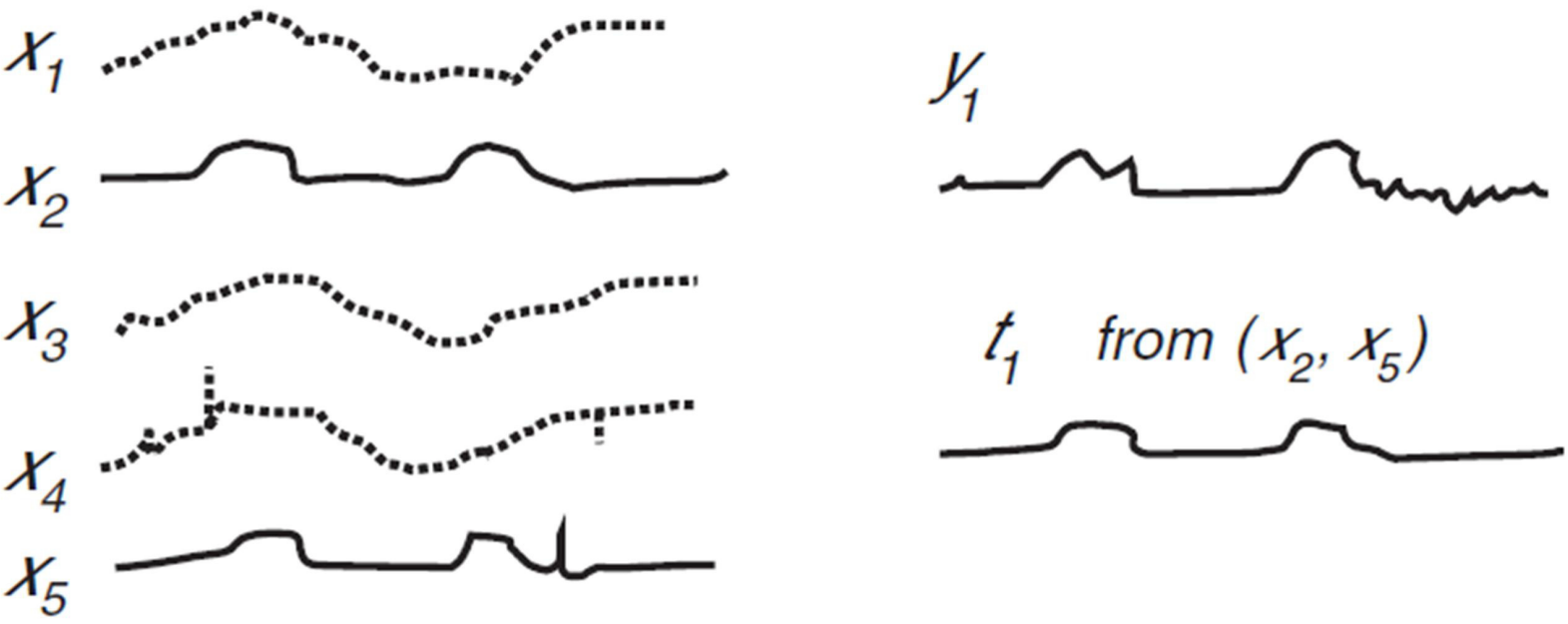

PARTIAL LEAST SQUARES (PLS)

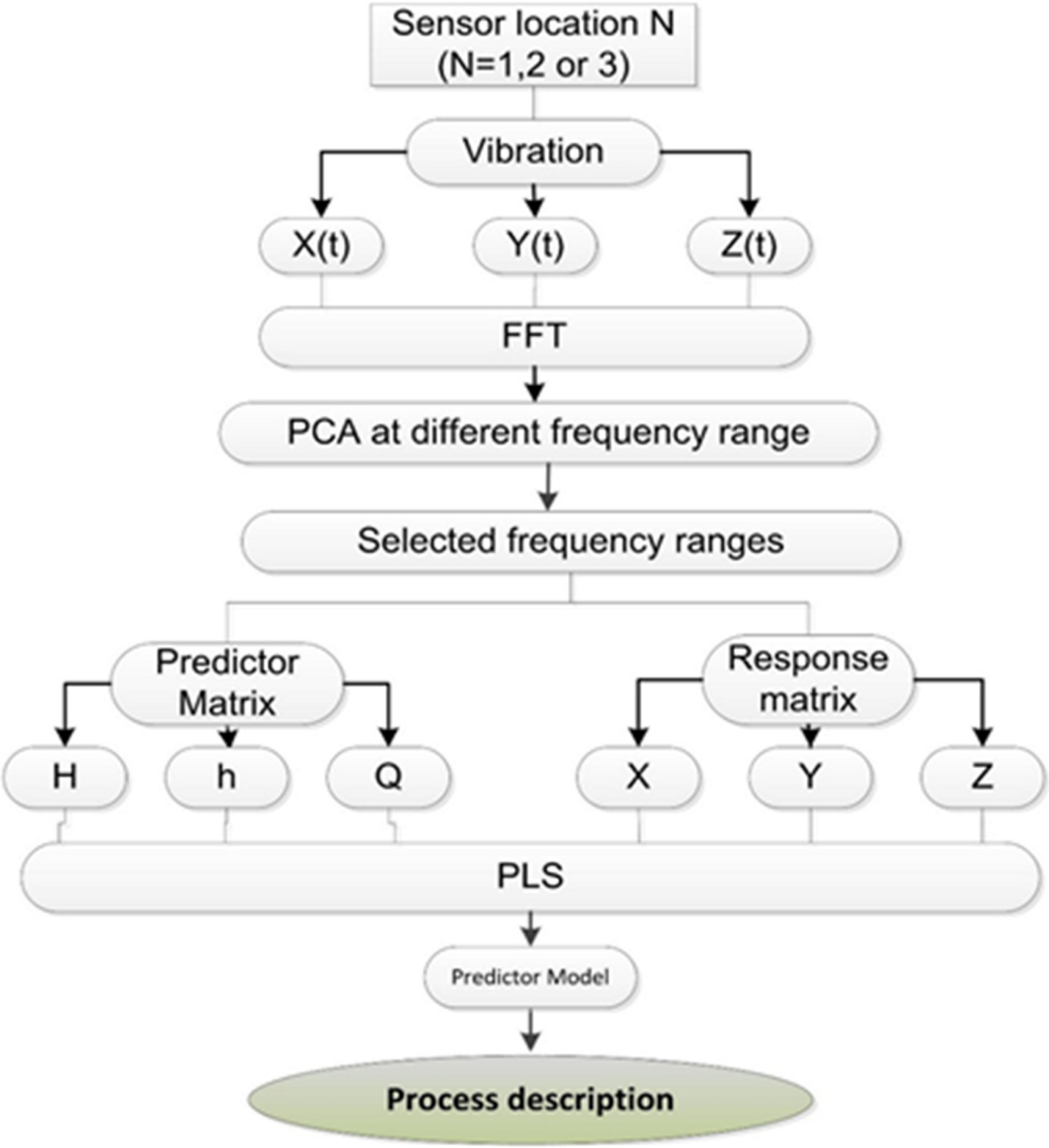
Sensor location N
(N=1,2 or 3)
Vibration
X(t)
Y(t)
Z(t)
FFT
PCA at different frequency range
Selected frequency ranges
Predictor
Matrix
Response
matrix
H
h
Q
X
Y
Z
PLS
Predictor Model
Process description

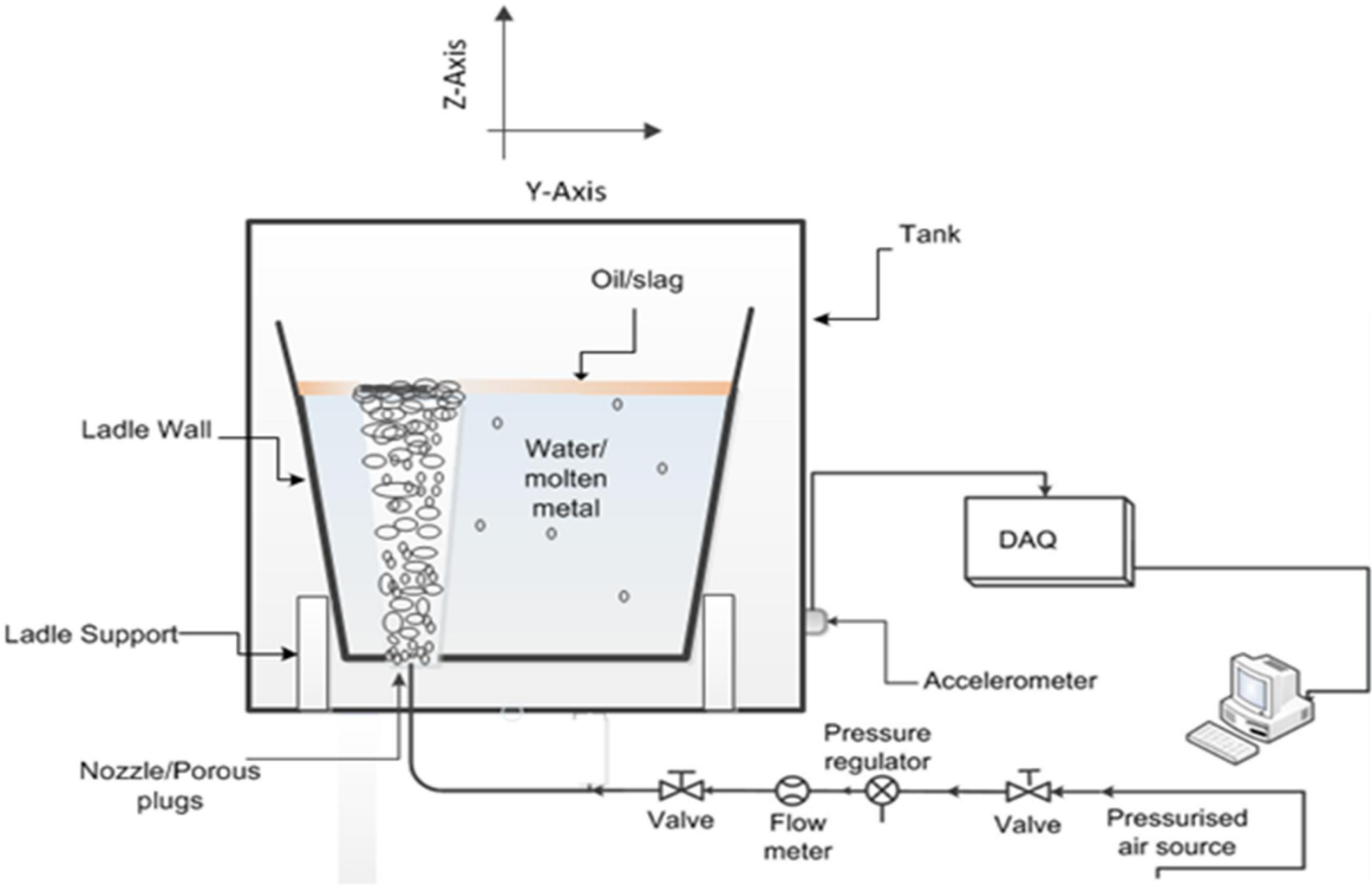
Z-Axis
Y-Axis
Tank
Oil/slag
Ladle Wall
Water/
molten
metal
DAQ
Ladle Support
Accelerometer
Pressure
regulator
Nozzle/Porous
plugs
Valve
Flow
meter
Valve
Pressurised
air source


Accelerometer

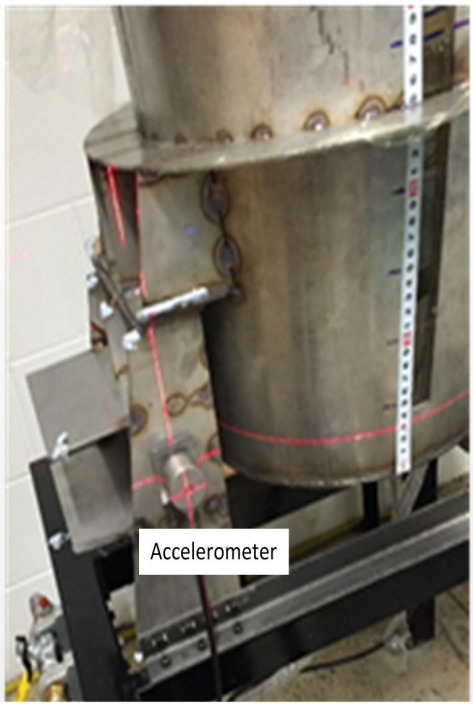
Accelerometer

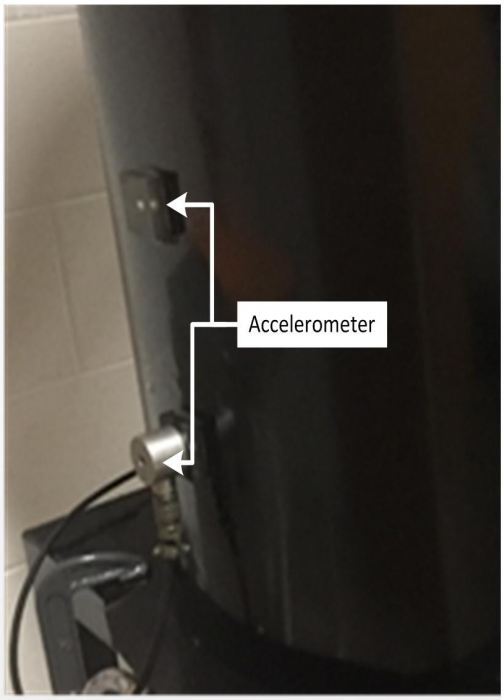
Accelerometer

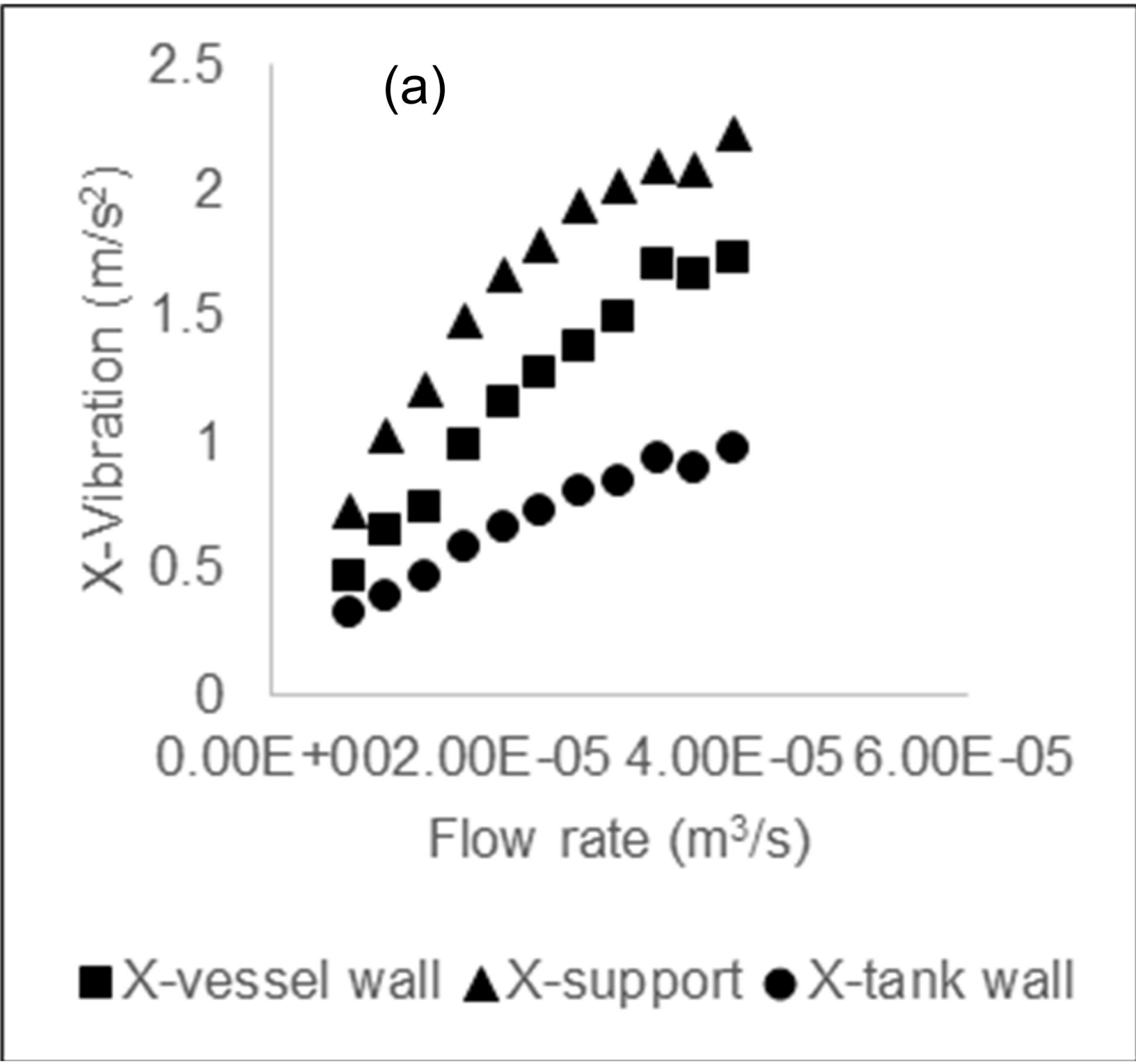
(a)
2.5
2
1.5
1
0.5
0
X-Vibration (m/s²)
0.00E+00
2.00E-05
4.00E-05
6.00E-05
Flow rate (m³/s)
X-vessel wall
X-support
X-tank wall

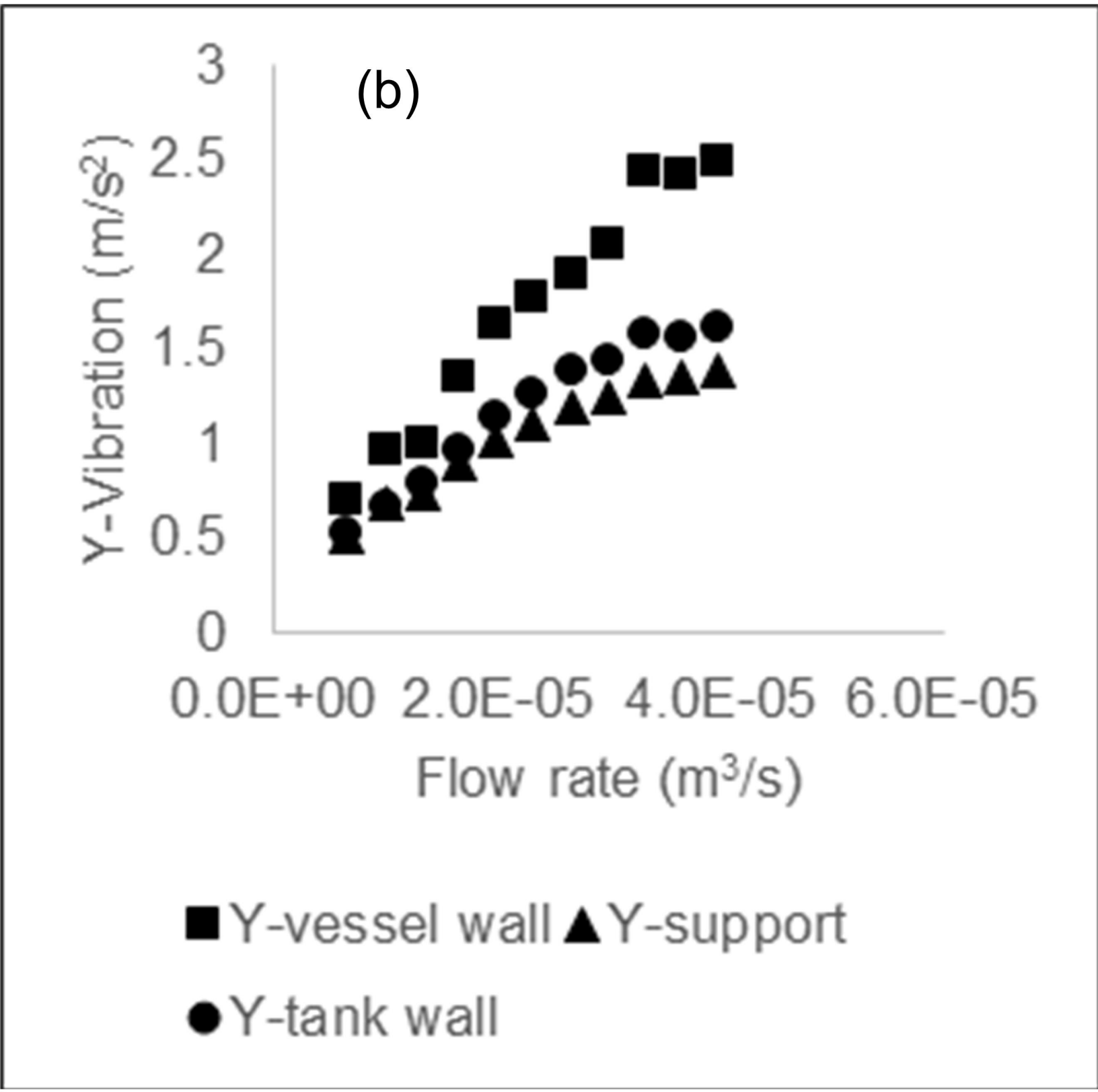
(b)
Y-Vibration (m/s²)
3
2.5
2
1.5
1
0.5
0
0.0E+00
2.0E-05
4.0E-05
6.0E-05
Flow rate (m³/s)
Y-vessel wall
Y-support
Y-tank wall

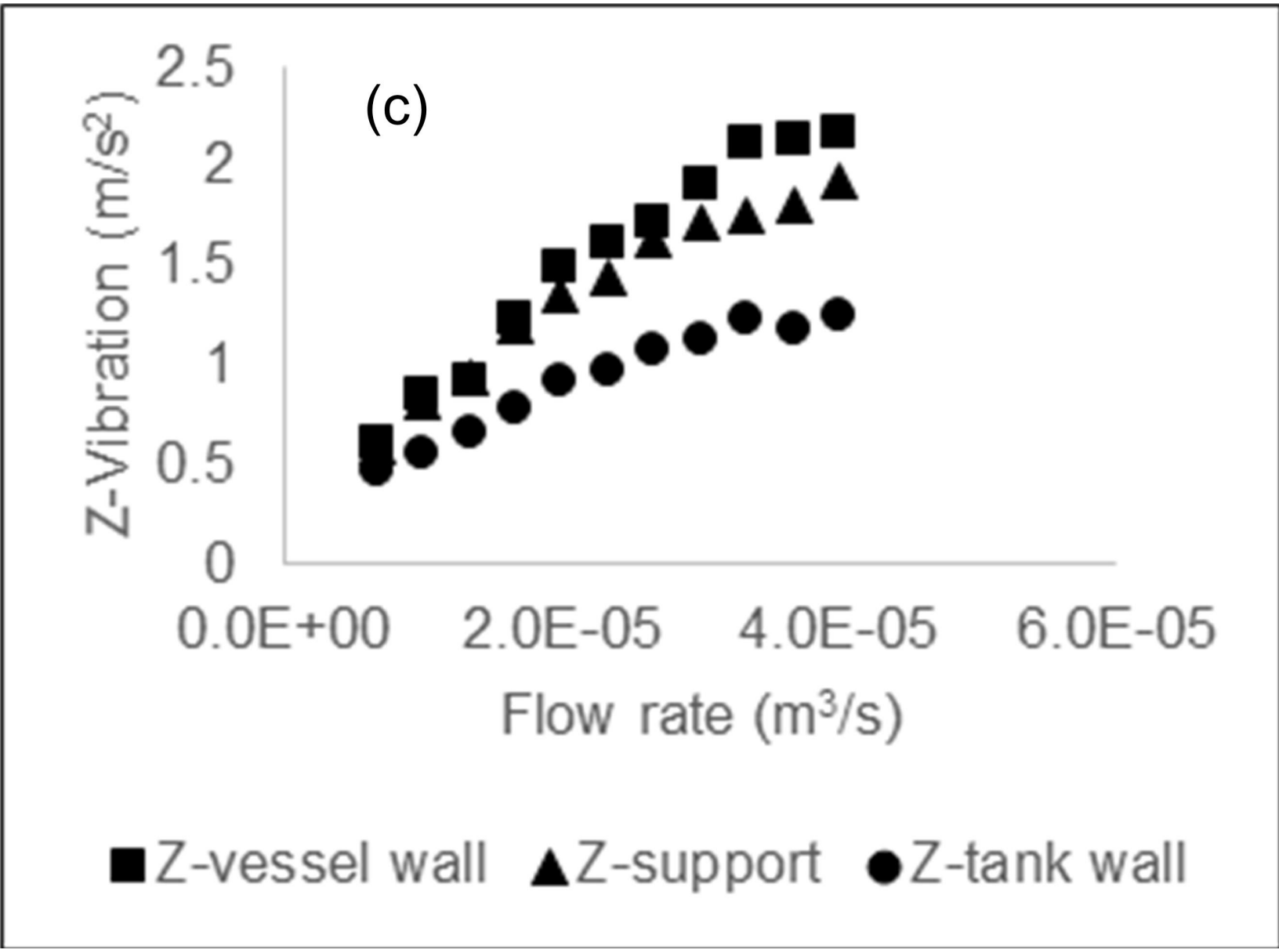
(c)
Z-Vibration (m/s²)
2.5
2
1.5
1
0.5
0
0.0E+00
2.0E-05
4.0E-05
6.0E-05
Flow rate (m³/s)
Z-vessel wall
Z-support
Z-tank wall

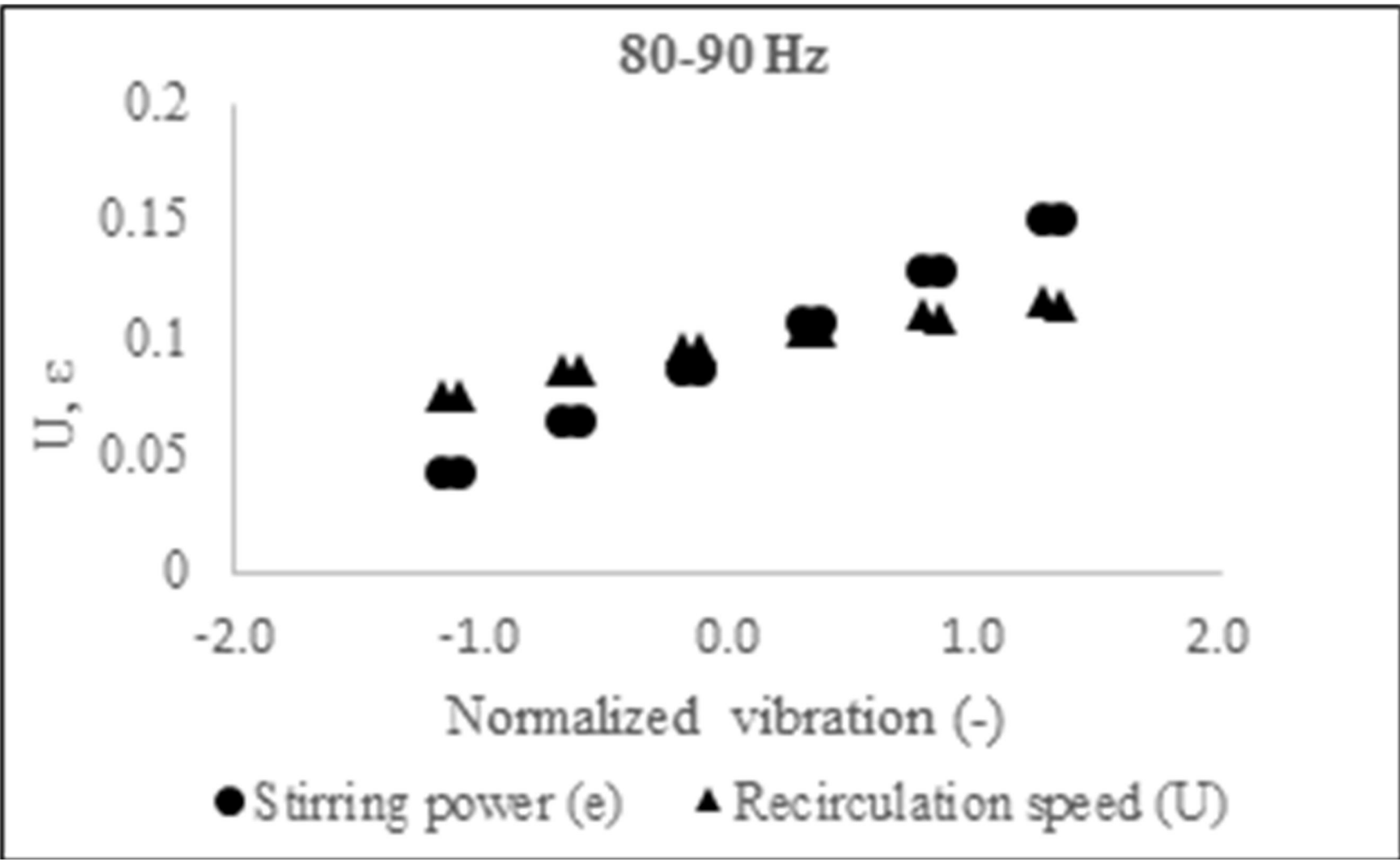
80-90 Hz
0.2
0.15
0.1
0.05
0
U, ε
-2.0
-1.0
0.0
1.0
2.0
Normalized vibration (-)
Stirring power (e)
Recirculation speed (U)

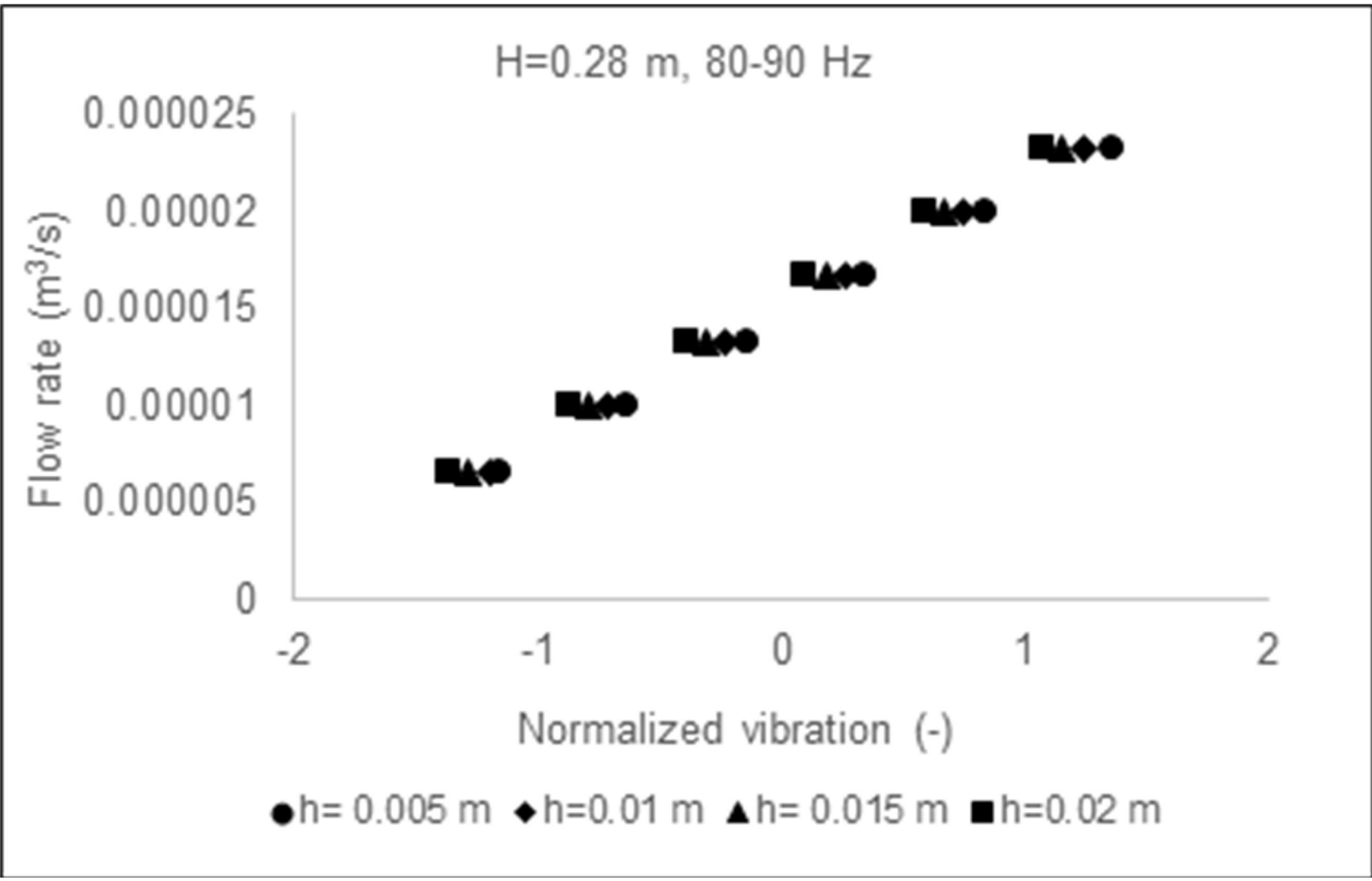
H=0.28 m, 80-90 Hz
0.000025
0.00002
0.000015
0.00001
0.000005
0
Flow rate (m3/s)
-2
-1
0
1
2
Normalized vibration (-)
h= 0.005 m
h=0.01 m
h= 0.015 m
h=0.02 m

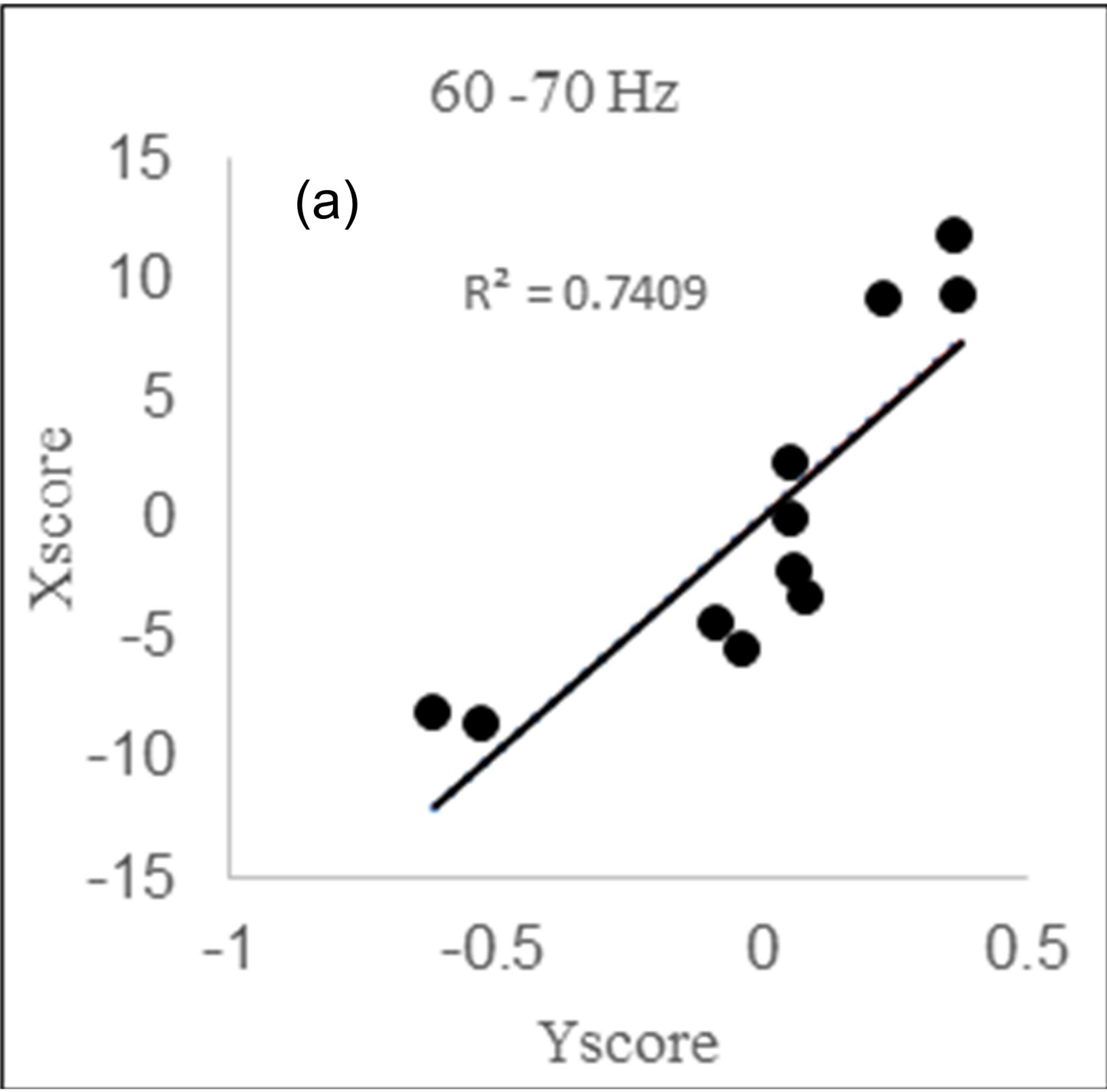
60 -70 Hz
(a)
R² = 0.7409
15
10
5
0
-5
-10
-15
Xscore
-1
-0.5
0
0.5
Yscore

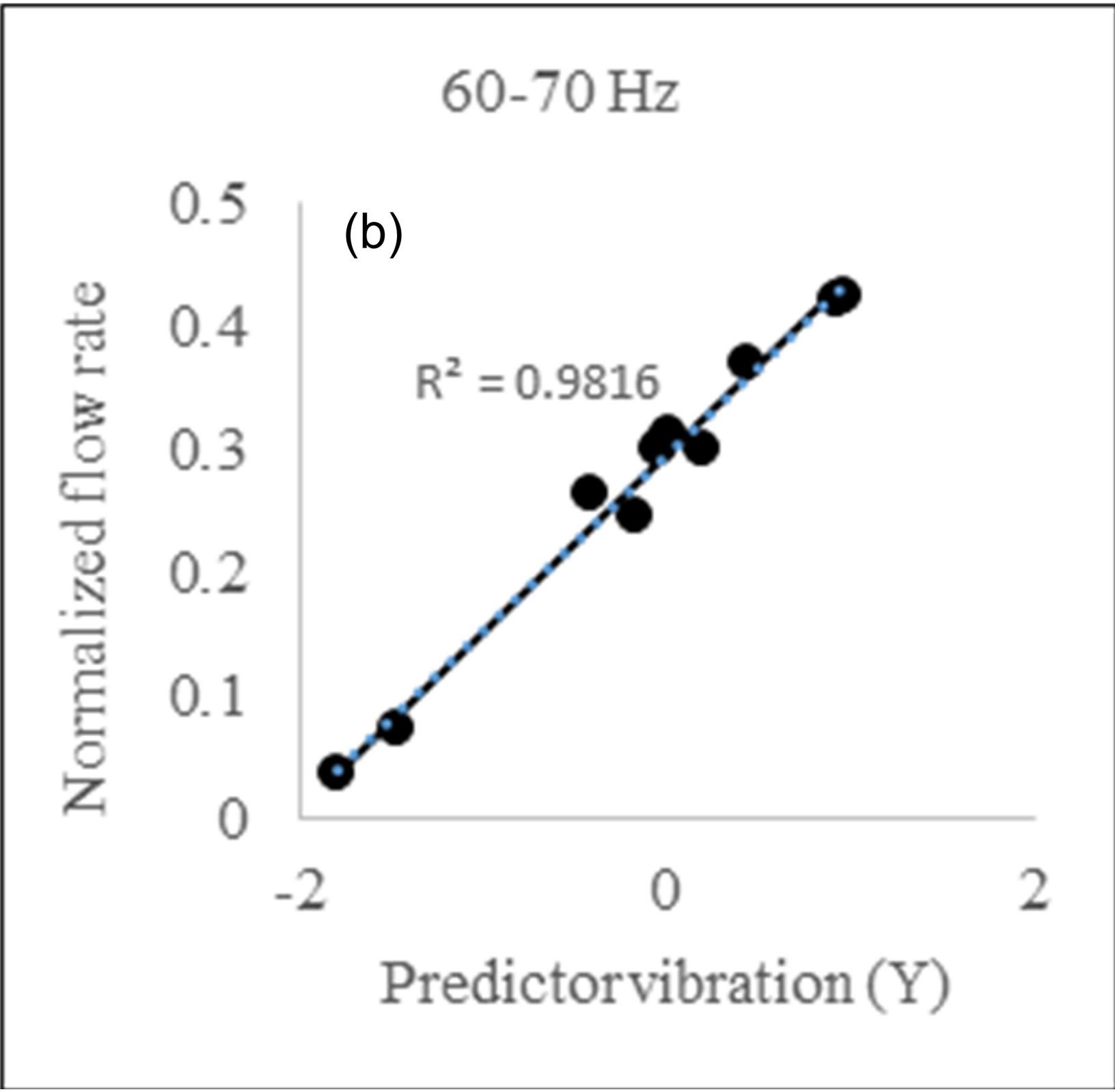
60-70 Hz
(b)
R² = 0.9816
Normalized flow rate
0.5
0.4
0.3
0.2
0.1
0
-2
0
2
Predictor vibration (Y)

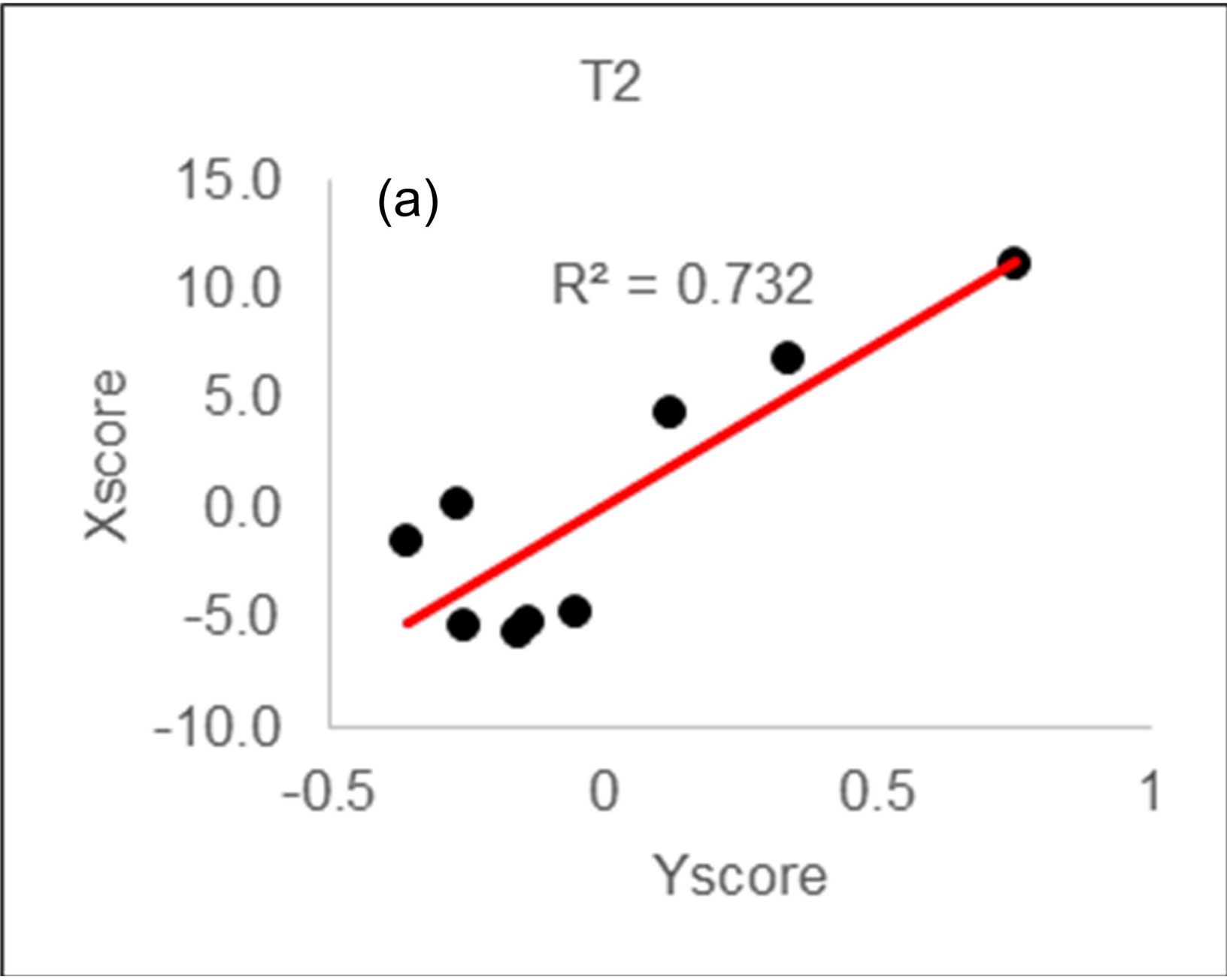
T2
(a)
R² = 0.732
15.0
10.0
5.0
0.0
-5.0
-10.0
Xscore
-0.5
0
0.5
1
Yscore

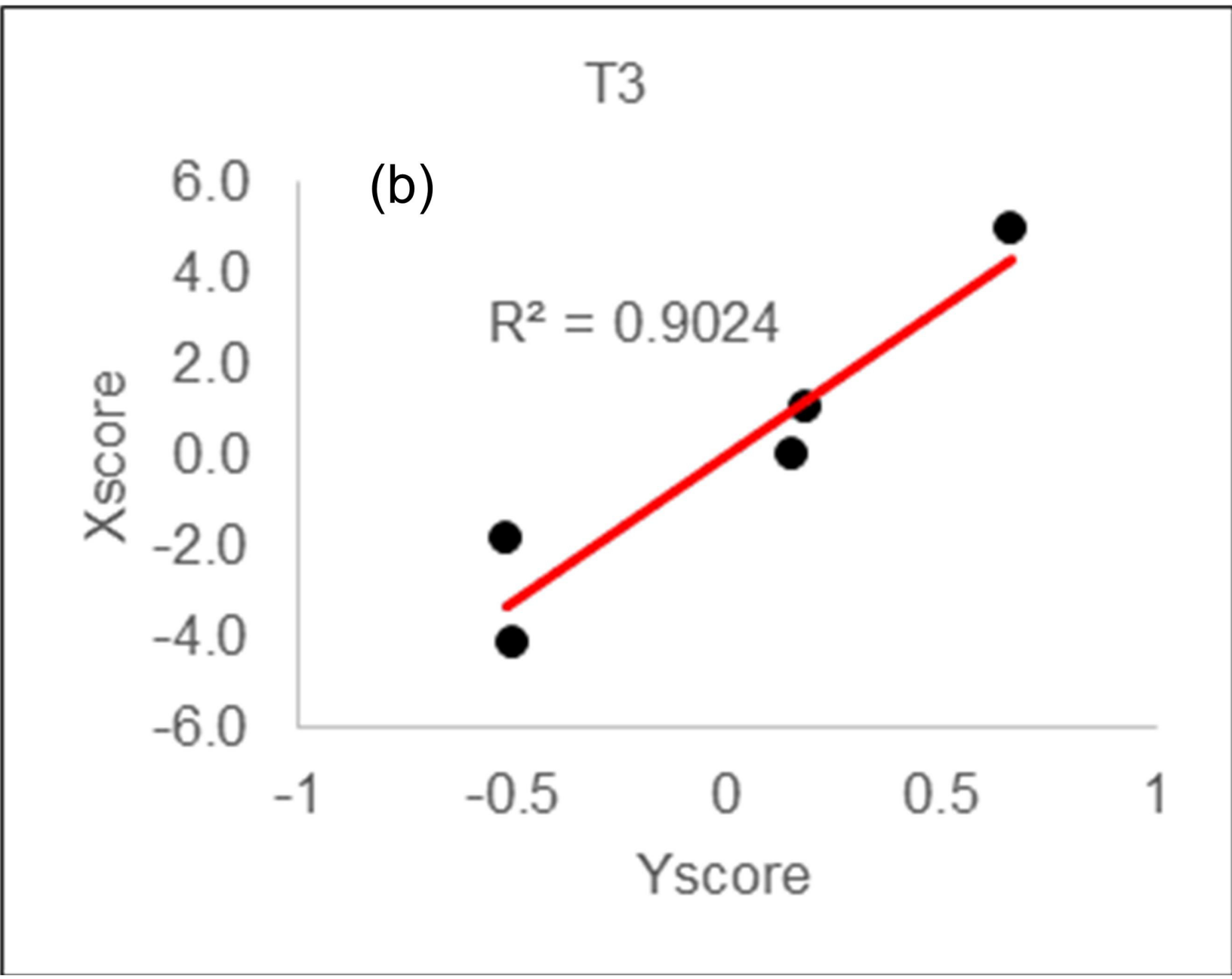
T3
(b)
6.0
4.0
2.0
0.0
-2.0
-4.0
-6.0
Xscore
R² = 0.9024
-1
-0.5
0
0.5
1
Yscore

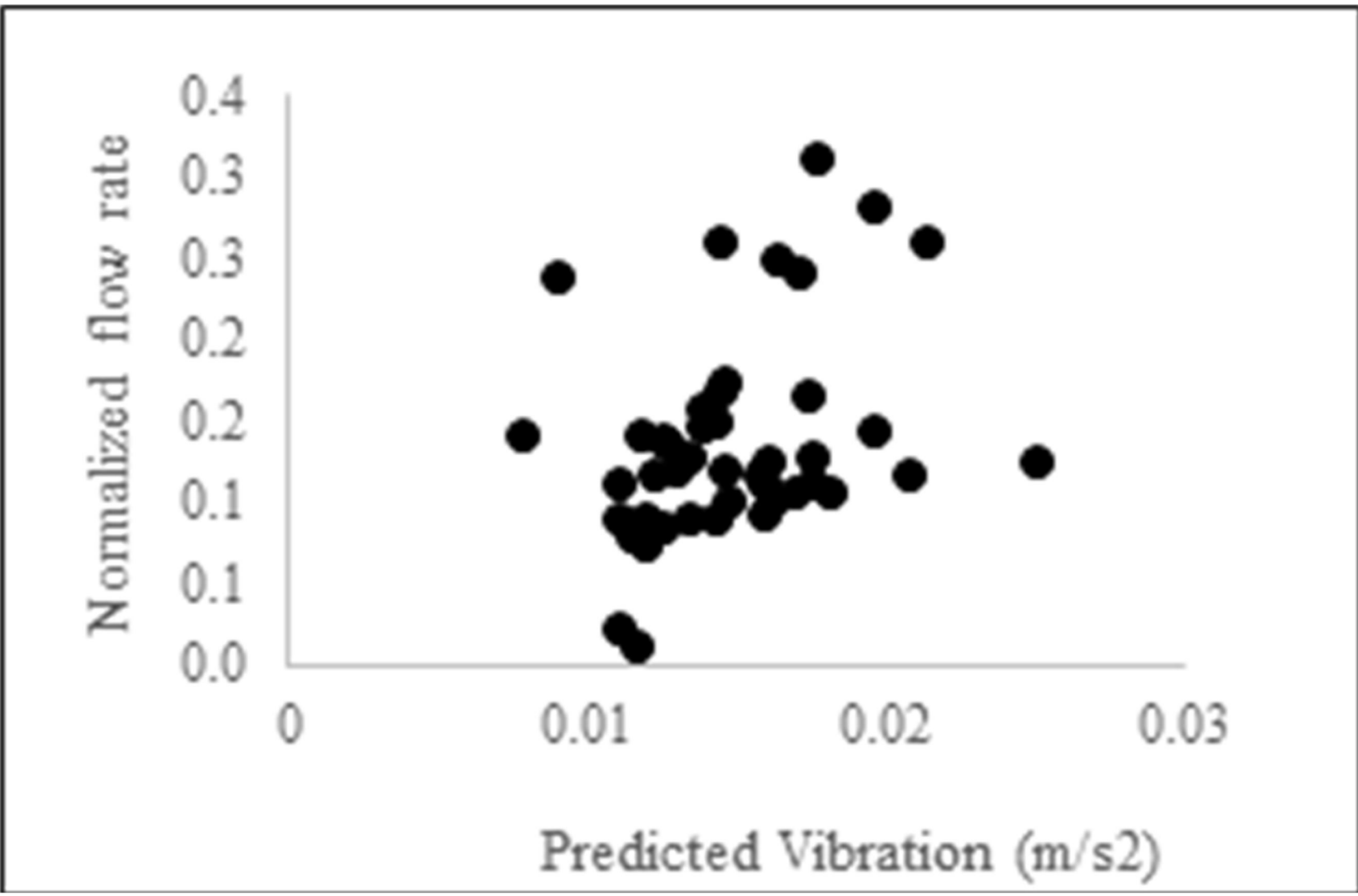
Normalized flow rate
0.4
0.3
0.3
0.2
0.2
0.1
0.1
0.0
0
0.01
0.02
0.03
Predicted Vibration (m/s2)

Tables

Table 1 PC1 values at different accelerometer locations.

Double layer	**Vessel Wall**	**Vessel support**	**Tank Wall**
Frequency range	90-100	90-100	150-160
PC1	99%	98%	99%
PC2	0.5	1	0.5

Table 2 PC1 and R^2 on the selected frequency ranges

Frequency range (Hz)		40-50	60-70	70-80	80-90	90-100
PC1		99.27	96.12	97.74	99.10	91.63
Parameters		R^2	R^2	R^2	R^2	R^2
R^2	PC1, ε	0.71	0.80	0.80	0.91	0.89
	PC1, U	0.72	0.82	0.66	0.88	0.87

Table 3 PC1 and PC2 values of four heats of the plant trial

Heat ID	**PC1 (%)**	**PC2 (%)**	**Frequency (Hz)**	**Heat ID**	**PC1 (%)**	**PC2 (%)**	**Frequency (Hz)**
T1	97	1	50-60	T3	80	16	50-60
	89	8	60-70		85	9	60-70
	86	10	70-80		70	12	70-80
	75	12	80-90		83	11	80-90
	92	3	90-100		87	5	90-100
	60	31	180-190		92	4	180-190
T2	94	4	50-60	T4	70	13	50-60
	97	2	60-70		88	10	60-70
	96	3	70-80		80	9	70-80
	98	1	80-90		82	13	80-90
	96	2	90-100		65	21	90-100
	93	1	180-190		62	31	180-190

Table 4 Comparison between cold model and plant trial results

Frequency (Hz)	**PC1 (%)**	
	Model	Plant
60-70	96.3	94
70-80	98	95
80-90	99	93
90-100	91	88